scientific reports

Check for updates

OPEN

# Development of novel canine phage display-derived neutralizing monoclonal antibody fragments against rabies virus from immunized dogs

Apidsada Chorpunkul[1], Usa Boonyuen[2], Kriengsak Limkittikul[3], Wachiraporn Saengseesom[4], Wallaya Phongphaew[5], Iyarath Putchong[5], Penpitcha Chankeeree[6], Sirin Theerawatanasirikul[7], Amin Hajitou[8], Surachet Benjathummarak[9], Pannamthip Pitaksajjakul[1,9], Porntippa Lekcharoensuk[6] & Pongrama Ramasoota[1,9]✉

**Animal rabies is a potentially fatal infectious disease in mammals, especially dogs. Currently, the number of rabies cases in pet dogs is increasing in several regions of Thailand. However, no passive postexposure prophylaxis (PEP) has been developed to combat rabies infection in animals. As monoclonal antibodies (MAbs) are promising biological therapies for postinfection, we developed a canine-neutralizing MAb against rabies virus (RABV) via the single-chain variable fragment (scFv) platform. Immunized phage-displaying scFv libraries were constructed from PBMCs via the pComb3XSS system. Diverse canine VHVLκ and VHVLλ libraries containing $2.4 \times 10^8$ and $1.3 \times 10^6$ clones, respectively, were constructed. Five unique clones that show binding affinity with the RABV glycoprotein were then selected, of which K9RABVscFv1 and K9RABVscFv16 showed rapid fluorescent foci inhibition test (RFFIT) neutralizing titers above the human protective level of 0.5 IU/ml. Finally, in silico docking predictions revealed that the residues on the CDRs of these neutralizing clones interact mainly with similar antigenic sites II and III on the RABV glycoprotein. These candidates may be used to develop complete anti-RABV MAbs as a novel PEP protocol in pet dogs and other animals.**

Rabies virus (RABV) is a neurotropic virus that causes rabies in mammals[1,2]. In particular, the RABV glycoprotein (RABV-G) can induce immune responses and is a major target for neutralizing antibodies[3,4]. It contains several antigenic sites: I, II, III, IV (G5) and minor site a (G1)[5–8]. Animal rabies is most prevalent in tropical countries such as Thailand, India, Bangladesh, and other Asian countries in Southeast Asia[9,10]. Thanapongtharm and colleagues reported that 9.9% (848/8,574 samples) and 15.4% (1475/9601) of animals in Thailand tested positive for rabies in 2017 and 2018, respectively. Most of the infected cases were dogs (87% of all positive samples), followed by cattle, cats, and others. More than half of these animals were domesticated, and many were unvaccinated animals (39%) that roam freely or semifreely. Rabies-positive dog clusters are concentrated in the northeastern region, followed by the central and southern provinces of Thailand. Notably, the number of cases increased after June and peaked in January[1].

[1]Department of Social and Environmental Medicine, Faculty of Tropical Medicine, Mahidol University, Bangkok 10400, Thailand. [2]Department of Molecular Tropical Medicine and Genetics, Faculty of Tropical Medicine, Mahidol University, Bangkok 10400, Thailand. [3]Department of Tropical Pediatrics, Faculty of Tropical Medicine, Mahidol University, Bangkok 10400, Thailand. [4]Queen Saovabha Memorial Institute (WHO Collaborating Center for Research on Rabies), Thai Red Cross Society, Bangkok 10330, Thailand. [5]Department of Pathology, Faculty of Veterinary Medicine, Kasetsart University, Bangkok 10900, Thailand. [6]Department of Microbiology and Immunology, Faculty of Veterinary Medicine, Kasetsart University, Bangkok 10900, Thailand. [7]Department of Anatomy, Faculty of Veterinary Medicine, Kasetsart University, Bangkok 10900, Thailand. [8]Cancer Phage Therapy Group, Department of Brain Sciences, Faculty of Medicine, Imperial College London, Hammersmith Hospital, London W12 0NN, UK. [9]Center of Excellence for Antibody Research, Faculty of Tropical Medicine, Mahidol University, Bangkok 10400, Thailand. ✉email: pongrama.ram@mahidol.ac.th

Although preexposure rabies vaccination effectively prevents disease in dogs, there is a risk of infection if the dog is not completely vaccinated[11,12]. Domesticated dogs can also be infected by strays with an unknown history of rabies vaccination[1,13,14]. In general, animals that develop symptomatic signs of rabies should be euthanized by an animal health professional, and the animal's head or fresh brain tissue should be submitted to the laboratory to confirm rabies virus infection[15].

The awareness of rabies has increased among pet owners in Thailand because it is a fatal disease caused by inflammation of the brain and spinal cord that can be transmitted from animals to owners[16]. Therefore, it is crucial to develop rabies-postexposure treatment or prevention approaches for companion animals, especially dogs. Biopharmaceuticals are promising potential treatments for animal rabies. Currently, studies on passive immunotherapies, such as monoclonal antibodies (MAbs), against rabies in domestic animals are lacking, whereas many human MAbs and commercialized anti-rabies virus immunotherapy products are being developed continuously[17–23]. Hence, this study aimed to develop therapeutic canine scFv monoclonal antibodies against rabies virus infection. On the basis of phage display technology, diverse canine scFv libraries were constructed from the PBMCs of immunized dogs. Anti-RABV glycoprotein scFv clones revealing high-binding signals were then selected for further investigation of their neutralizing activity against RABV. Finally, in silico models were used to predict the interactions between candidate antibodies and the RABV glycoprotein by docking experiments.

## Results

### Anti-rabies virus immunization in dogs and evaluation of canine serum antibody titers via the immunoperoxidase monolayer assay (IPMA)

On day 0, all the serum samples presented the highest antibody titer at a ratio of 1:10, whereas, samples taken on the same day (no. 3, 6, 7, 10, and 12) presented mild antibody responses. Three weeks after the first dose, all the sera except those from groups 3, 6, 10, and 12 presented higher antibody titers than did those from the first immunization at a ratio of 1:100. Three weeks after the second vaccination (day 42), all the samples exhibited a mild antibody response at a ratio of 1:1000 (Fig. S1). Accordingly, 13 dogs received a booster three weeks after the third dose, and blood samples were collected two weeks after this booster.

### Measurements of serum-neutralizing antibody titers against the rabies virus via the rapid fluorescent foci inhibition test (RFFIT)

Individual sera were collected for two weeks after the last booster and tested for neutralizing antibody titers against the rabies challenge virus standard (CVS) strain via the RFFIT assay. The levels of neutralizing antibodies ranged from 17 to 60 IU/ml (Fig. 1), which were higher than the protective level of 0.5 IU/ml. Two dogs showed high antibody responses, which were greater than 50 IU/ml.

### Variable heavy chain (VH) and variable light chain (VL) fragments amplification

PBMCs were separated from all blood samples, and total RNA was extracted. The pooled RNA samples were then converted to cDNA. The synthesized cDNA served as PCR templates for VH and VL fragment amplifications using specific primers for the canine pComb3XSS-scFv antibody (detailed in the Materials and Methods). The sizes of the VH and VL PCR products and the purified products were approximately 450 and 350 bp, respectively (Fig. 2).

### Single-chain variable fragment (scFv) library constructions

Sixteen clones from each library were randomly selected. The results revealed a cloning efficiency of 100% (16/16) for the VHVLκ library and 75% (12/16) for the VHVLλ library (Fig. 3). The VHVLκ and VHVLλ libraries consisted of $2.4 \times 10^8$ and $1.3 \times 10^6$ clones, respectively.

### Determination of scFv library diversity via BstNI analysis

The diversity of the constructed libraries was determined via BstNI analysis (Fig. 4). The patterns of the DNA fingerprints of 30 random clones from the VHVLκ and VHVLλ non-panning libraries completely differed across groups.

### Affinity selection (Biopanning)

Purified inactivated rabies virus (RABV) and recombinant glycoprotein of rabies virus (rG) were used as target antigens to screen and obtain scFv clones with binding activity from either the VHVLκ or VHVLλ library. Figure 5 shows the results of the affinity binding selection for both anti-rG and anti-RABV. The overall input titers of the VHVLκ and VHVLλ libraries were approximately $10^{10}$ – $10^{11}$ CFU/ml. Target-bound phages were enriched in the output titer. Titers slightly increased in successive rounds (2nd–4th rounds) of the panning selection procedure for all experiments except for the anti-rG binding outputs of the VHVLκ library.

For the VHVLκ anti-rG binding tests, the outputs of the second round were slightly higher than those of the first round. Compared with that of the second round, the third-round output slightly decreased, and the fourth-round output phage titer was 10 times higher than that of the third round. Compared with that in the first round, the target-bound phage titer in the VHVLκ library in the anti-RABV binding tests slightly decreased. The titers tended to increase in the third panning, and the titer increased 10-fold in the fourth output.

In the anti-rG binding test of the VHVLλ library, the third output titer was 10 times higher than the second, and the fourth output titer was 10 times higher than the third titer. In the anti-RABV binding test of the VHVLλ library, the titer of the third output phage was 10 times higher than that of the second round, but the titer of the fourth output was similar to that of the third.

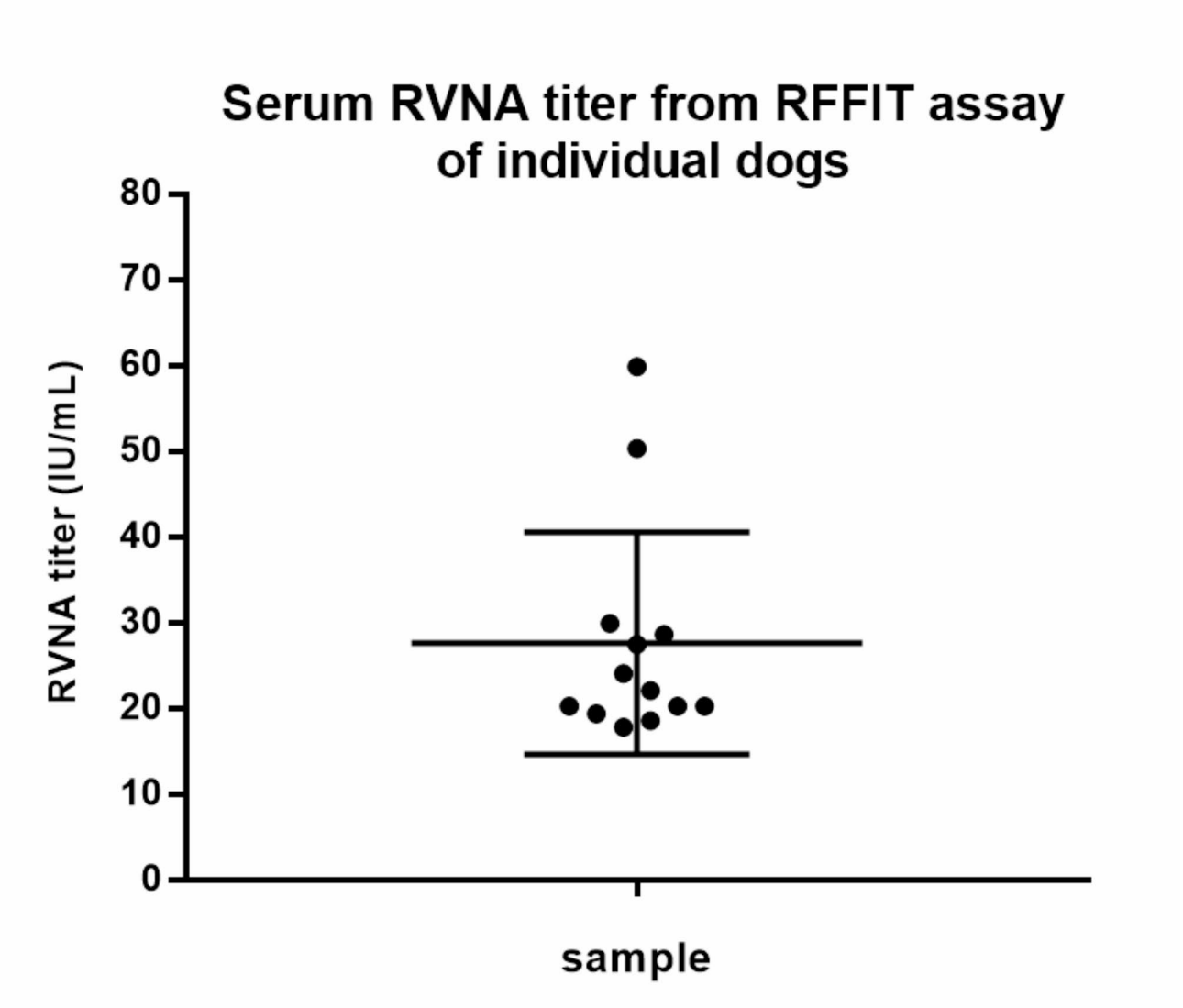


**Fig. 1**. Serum VNA titer against rabies virus in dogs via the RFFIT assay. All 13 serum samples presented neutralizing antibody levels greater than 0.5 IU/ml. The average titers ranged from 20 to 30 IU/ml. Two outliers presented levels greater than 50 IU/ml.

## ELISA screening of individual canine scFv clones

Pooled phage clones (TG1) with RABV binding affinity were collected during biopanning; individual clones were subsequently obtained via ELISA. Fifty-eight phage clones from the fourth-round output plates were randomly chosen. Clone numbers 1–19, 20–37, and 38–58 are shown in Fig. 6a–c, respectively. The inactivated RABV binding signals of 33 out of 58 clones (clones no. 1–6, 10–18, 36, 37, 39, 41–46, 49, and 51–58; *) were significantly greater than those of the negative control. Twenty-five unselected clones were excluded from further characterization. The negative control binding signals of 19 clones (clones no. 7, 8, and 19–35; #) were greater than the target binding signals, and the signal levels of the other six clones (9, 38, 40, 47, 48, and 50; 'NS' symbol) were not significantly different from those of the negative control.

Thirty-six soluble scFv antibodies from 58 clones (numbers 1–6, 9–18, 36–46, 49, and 51–58; *) significantly bound to rG. Nineteen clones were unselected (7, 8, and 19–35; #) because the rG binding signals were lower than the SM binding signals, or the inactivated RABV binding signals of some positive rG binding clones were lower than those of the negative control. The antigen binding signals of the other three unselected clones (47, 48, and 50; "NS" symbol) were not significantly different from those of the SM control.

Finally, only 20 scFv clones (numbers 1–6, 10–17, 36, 37, 39, 44, 54, and 58) presented either inactivated RABV or recombinant RABV-G binding signals, which were significantly different, with P values $\leq 0.01$ (**) or $\leq 0.001$ (***), from those of the SM control. ELISA clones no. 1–6, 12, 16, 36, 39, 44, and 54 were from the VH-VLκ output, whereas clones no. 15, 37, and 58 were from the VH-VLλ output library. All these antibodies were determined, and miniprep plasmid purifications were performed for further DNA sequencing characterizations.

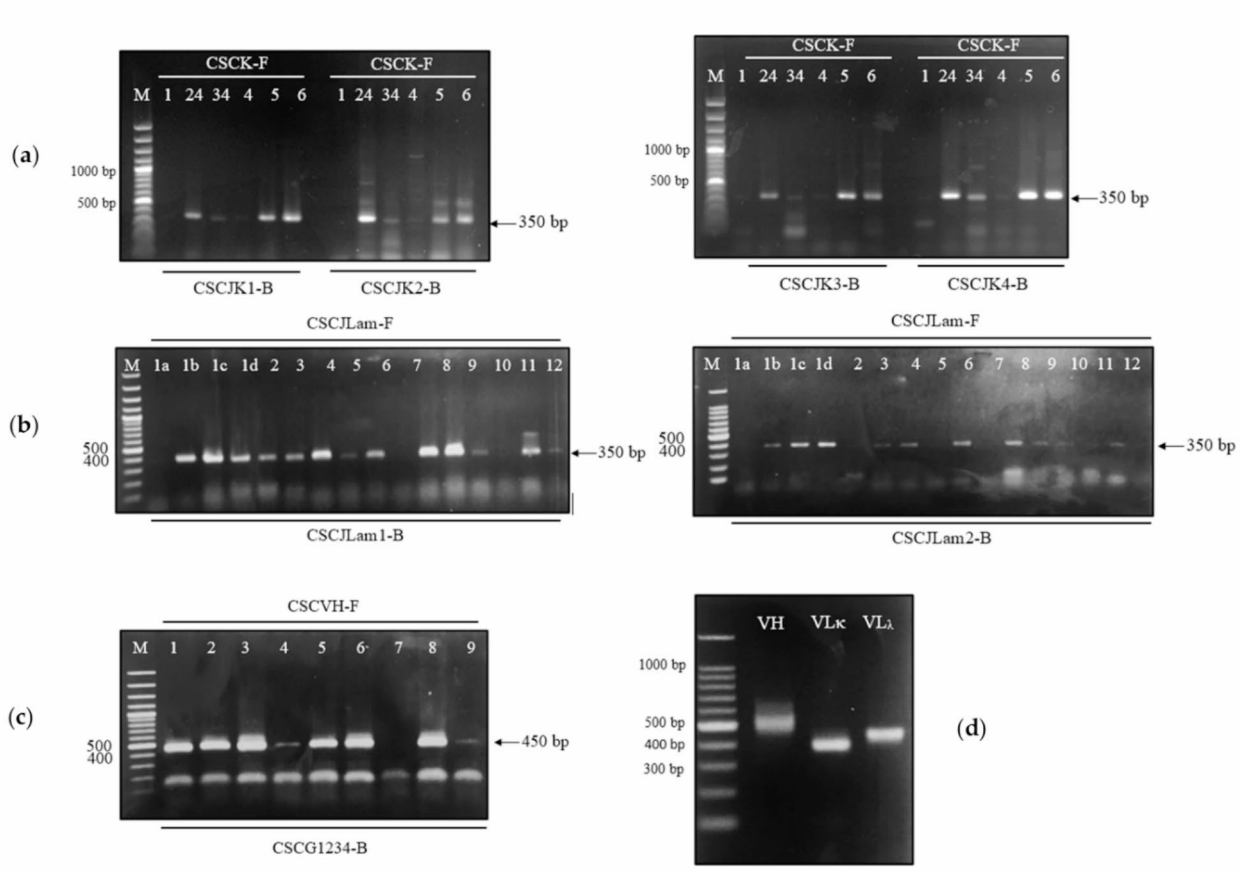


**Fig. 2**. VH, VLλ, and VLκ amplification via conventional PCR. (**a**) VLκ amplicons were amplified via sets of forward primers (CSCK1-F, 24-F, 34-F, 4-F, 5-F, and 6-F; numbers 1, 24, 34, 4, 5, and 6 in the figure). Four reverse primers were used: CSCJK1-B, CSCJK2-B, CSCJK3-B, and CSCJK4-B. (**b**) VLλ amplicons were amplified via sets of forward primers (CSCLam1a-F–CSCLam13-F; numbers 1a, 1b, 1c, 1d, and 2–13 in the figure). CSCJLam1-B and CSCJLam2-B served as reverse primers. The size of the VLκ and VLλ PCR products was 350 bp. (**c**) VH amplicons were amplified via the forward primer (CSCVH1-F–CSCVH9-F; numbers 1–9 in the figure) and the CSCG1234-B reverse primer. The size of the VH PCR products was 450 bp. (**d**) Purified variable chain fragments. After the antibody fragments were amplified via PCR, the corrected PCR products were purified via gel extraction (Lane 1, purified VH; Lane 2, purified VLλ; and Lane 3, purified VLκ). The PCR products were run on 1.2% agarose gels.

## DNA sequencing and amino acid translation

DNA from 20 ELISA-specific binding clones was sequenced; corrected full-length DNA sequences of canine scFv antibodies (approximately 800–850 bp) were observed for all antibodies except for two clones (nos. 36 and 37) whose 550-bp DNA sequences of VH fragments and linkers were incomplete. The full scFv DNA sequences were further analyzed via IMGT data (IMGT/V-QUEST; https://www.imgt.org/IMGT_vquest/analysis) for *Canis lupus familiaris* antibodies. Among the 18 sequences, only nine amino acid sequence patterns (named K9RABVscFv1, 2, 12, 15, 16, 39, 44, 54, and 58) were categorized on the basis of combinations of different amino acid sequences in complementarity-determining regions (CDRs)-1, -2, and −3 of the VL and VH fragments. ELISA clones no. 1, 3, 4, 5, 10, 11, and 13 contained the same CDR amino acid sequences and were named K9RABVscFv1. ELISA clones no. 2, 6, and 17 were K9RABVscFv2. ELISAs revealed that clones no. 12 and 14 were K9RABVscFv12, whereas clones no. 15, 16, 39, 44, and 58 were K9RABVscFv15, K9RABVscFv16, K9RABVscFv39, K9RABVscFv44, and K9RABVscFv58, respectively. We subsequently performed a pilot RFFIT neutralization assay of nine unpurified soluble scFvs in PBS (TG1 *E. coli*) before performing large-scale protein expression and purification for neutralization testing of the purified scFv (Table S1). Five clones (K9RABVscFv1, K9RABVscFv2, K9RABVscFv12, K9RABVscFv15, and K9RABVscFv16) with superior neutralization ability were selected because their neutralization ability tended to be high. The amino acid sequences and alignments are shown in Table S2 and Fig. 7, respectively. The complementarity-determining regions (CDRs) and frameshift region amino acid sequences of the variable chains are also shown in Fig. 7. IMGT database analysis revealed that the variable light chains of K9RABVscFv clone numbers 1, 2, 12, and 16 were the kappa subtype, whereas only clone number 15 was the lambda subtype. Because of randomized combinations of VH and VL fragments, the CDRs of individual antibodies mostly manifested with different amino acid sequences. However, some CDRs

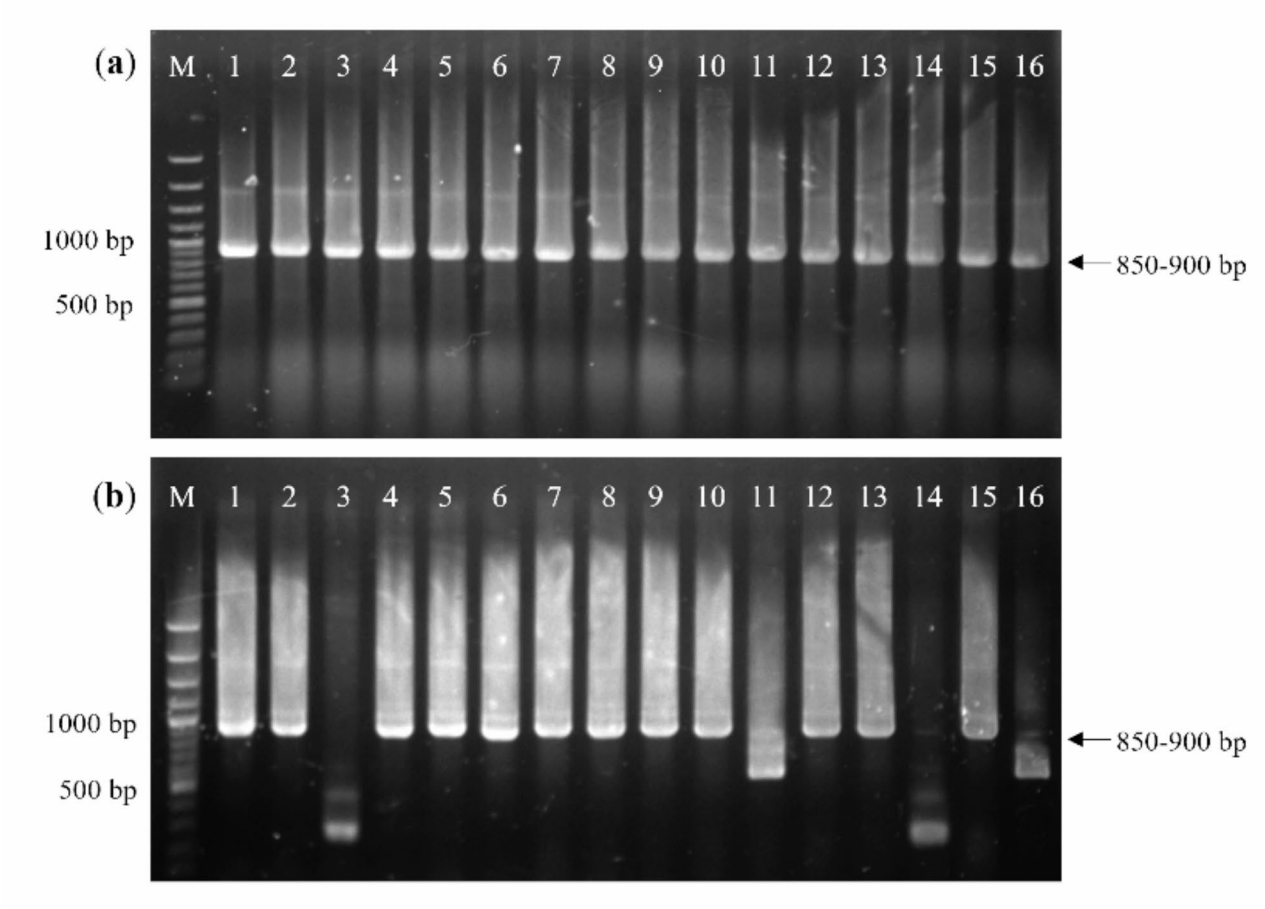


**Fig. 3**. Colony PCR of 16 randomly selected clones from the (**a**) VHVLκ scFv library and (**b**) VHVLλ scFv library. The inserted scFv antibodies were amplified via second-round PCR primers (RSC-F and RSC-B(AA) primers), and the size of the PCR product was 850–900 bp, as observed on a 1% agarose gel. M refers to the 100 bp DNA ladder.

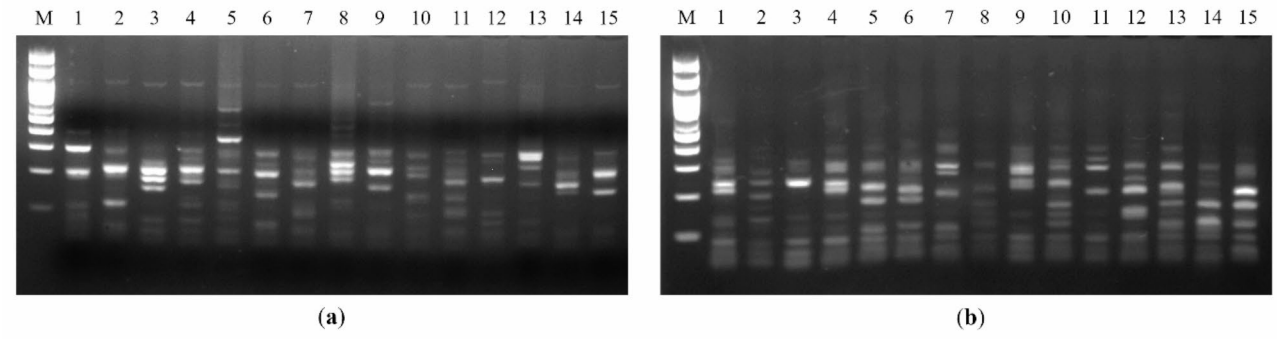


**Fig. 4**. BstNI analysis of the scFv libraries. (**a**) Fingerprint BstNI digestion of 15 randomly selected clones from the VHVLκ library. (**b**) Fifteen randomly selected clones from the VHVLλ library.

containing patterns similar to those of clones K9RABVscFv1, 2, 15, and 16 shared the same CDR1 amino acid sequences on VL chains (QSLLHSNGNTY). Only one residue on CDR1-VL of K9RABVscFv12 was dissimilar to that of the other clones (QSLLHSDGNTY). CDR2-VL of K9RABVscFv2 and 15 had the same sequence, "QVS," whereas the "KVS" sequence was observed in K9RABVscFv12 and 16. A unique "AVS" sequence was found in the CDR2-VL of K9RABVscFv1.

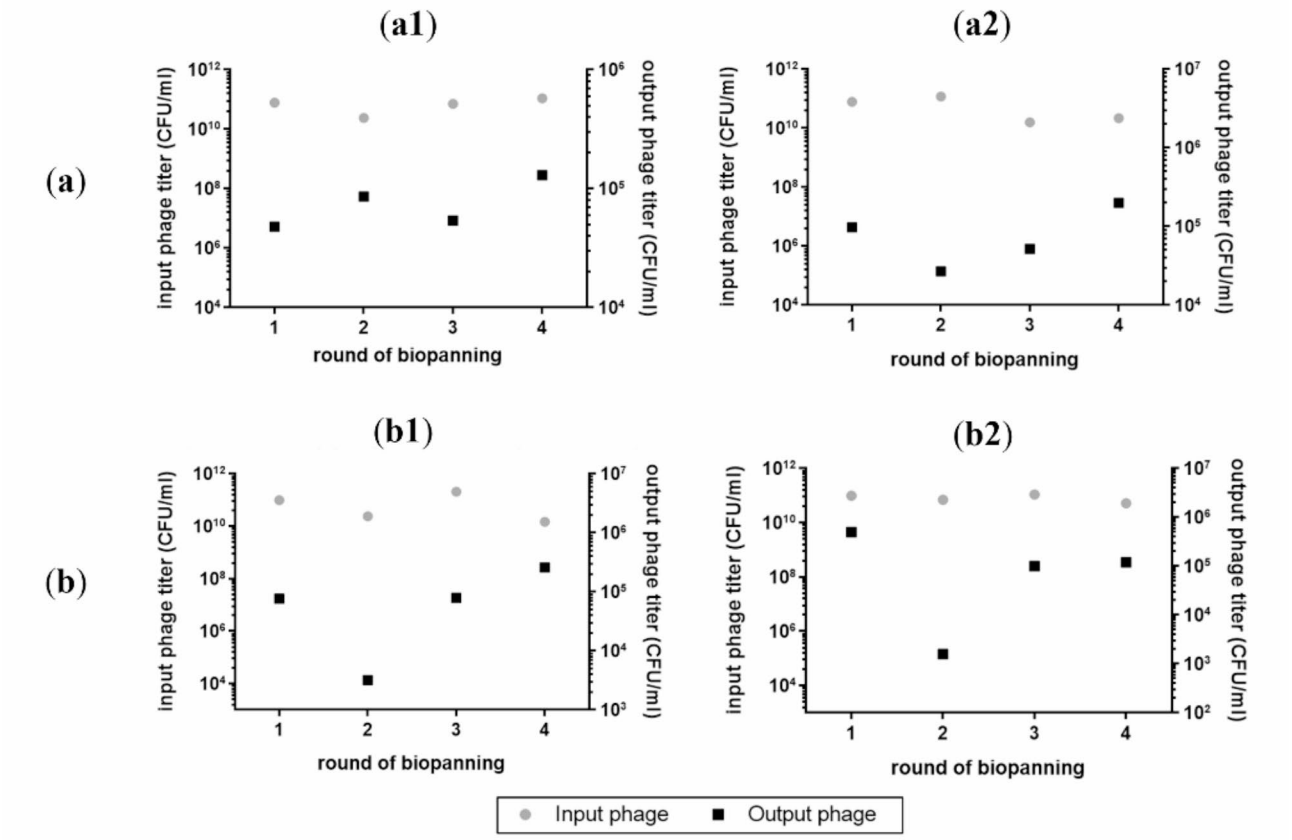


**Fig. 5**. Input and output phage titers (CFU/ml) of the (**a**) VHVLκ and (**b**) VHVLλ libraries. Four selection rounds were performed per target antigen. The results of the affinity selection process are shown in the scatter plots. (**a1**) (**b1**) rG binding selection. (**a2**) (**b2**) RABV binding selection. The Y-axis shows the power of ten logarithmic scales, the left side indicates the input titers, and the right side indicates the output titers. The gray and black dots indicate the input and output phage titers of each round, respectively.

*Germline immunoglobulin repertoire characterization*

The immunoglobulin germline repertoires of the five K9RABVscFv clones were investigated via IMGT reference allele databases. Table 1 shows the results for the germline genes and families in the V region of CDR3. VL-VH scFv revealed that pairing of the IGKV2-IGHV3 canine antibody germline family was predominant (4/5 clones; K9RABVscFvs no. 1, 2, 12, and 16), whereas VL-VH pairing of the IGLV2-IGHV3 family was discovered in K9RABVscFv15. Analysis of the V-alleles of VH revealed a predominance of the IGHV3-5*01 allele (clone numbers 1, 2, and 12), followed by IGHV3-6*01 (clone no. 15) and IGHV3-41*01 (clone no. 16). All the scFv clones used the same IGHJ4*01 (VH) and IGKJ1*01 (VL) alleles, except for the IGLJ2*01 allele for K9RABVscFv15.

## Soluble K9RABVscFv production, purification, and concentration

The results of the western blot analyses of the concentrated K9RABVscFv clones are presented in Fig. 8. The total protein concentrations of the purified K9RABVscFv clones were measured with a Pierce BCA Protein Assay Kit (Thermo Scientific), and the absorbance at 560 nm was as follows: K9RABVscFv1 (5.35 and 7.35 mg/ml), K9RABVscFv2 (6.12 mg/ml), K9RABVscFv12 (4.08 mg/ml), K9RABVscFv15 (4.30 mg/ml), and K9RABVscFv16 (5.88 and 7.11 mg/ml).

The binding ability of these five purified K9RABVscFv clones was assessed via ELISA. Five hundred nanograms of inactivated RABV were coated on the bottom ofeach well, and 100 µl of individually purified and concentrated scFv antibodies (0.6 µg/µl) were added to each well. ELISA signals were measured by absorbance at 450 nm (Fig. 9). K9RABVscFv1 presented the highest binding signal, followed by K9RABVscFv15, K9RABVscFv2, K9RABVscFv16, and K9RABVscFv12. All the clones were significantly different from the BSA-negative control.

## RFFIT neutralization activity of the purified K9RABVscFv clones

Seven purified K9RABVscFv samples consisting of K9RABVscFv1_1 (5.35 mg/ml), K9RABVscFv1_2 (7.35 mg/ml), K9RABVscFv2 (6.12 mg/ml), K9RABVscFv12 (4.08 mg/ml), K9RABVscFv15 (4.30 mg/ml), K9RABVscFv16_1 (5.88 mg/ml), and K9RABVscFv16_2 (7.11 mg/ml) were tested for rabies virus neutralizing antibody activity (RVNA) via the RFFIT assay. K9RABVscFv1 and K9RABVscFv16 showed

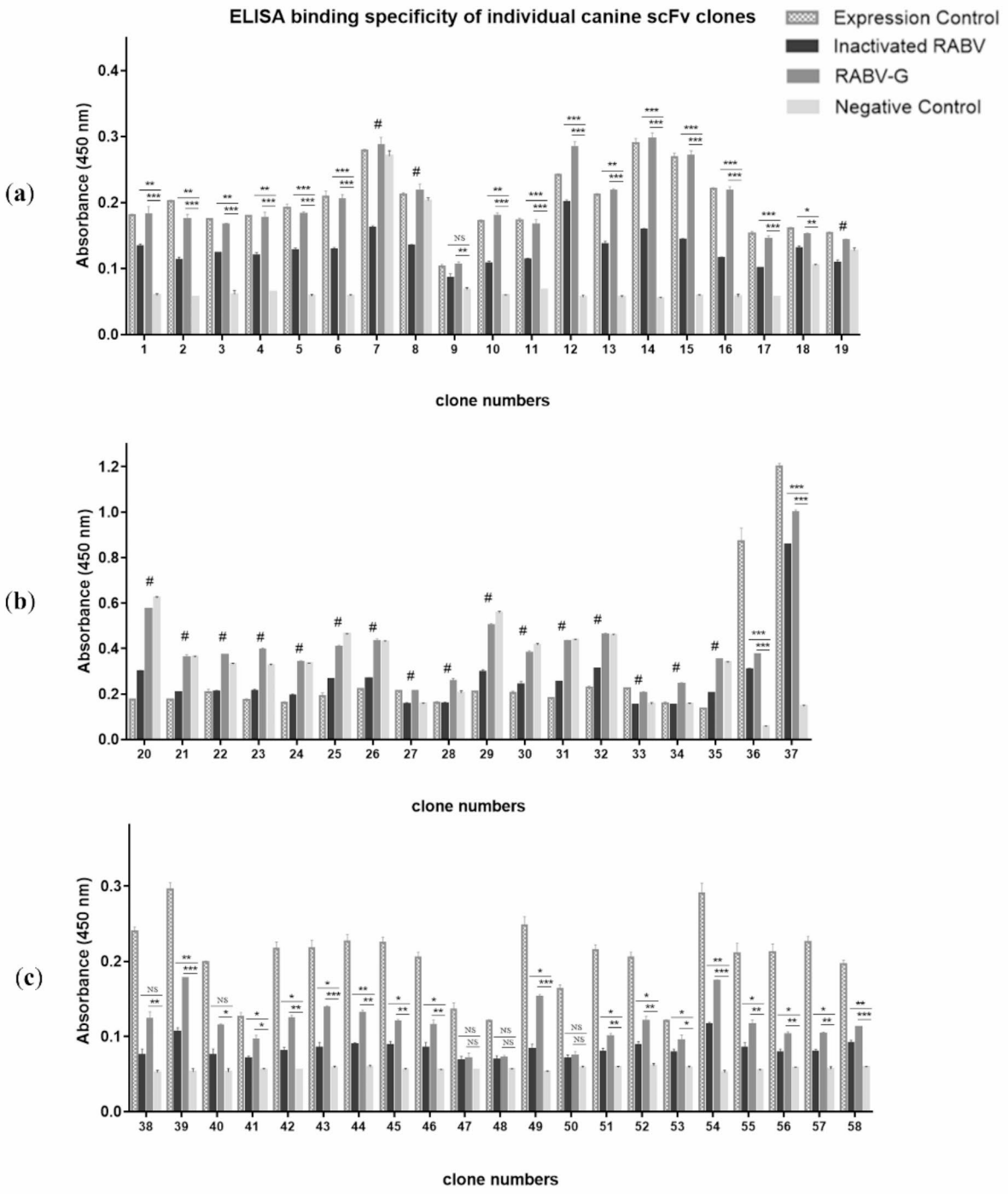


**Fig. 6**. ELISA absorbance signal at 450 nm from soluble fractions of all 37 clones. Each sample consisted of four wells: expression control, RABV, rG, and negative control (SM). (**a**) Clone numbers 1–19. (**b**) Clone numbers 20–37. (**c**) Clone numbers 38–58. Differences between the absorbance levels of the target antigens and SM binding were assessed via independent t tests. The asterisks indicate significant differences as follows: *P* value ≤ 0.05 (*), ≤ 0.01 (**), and ≤ 0.001 (***). The symbol "#" refers to an excluded sample whose signal from the negative control was greater than or equal to that of the scFv samples. A secondary anti-HA-conjugated HRP antibody bound to the scFv was detected using a TMB substrate. The error bars indicate the SDs of two replicates.


**Fig. 7**. Amino acid sequence alignments for the five selected K9RABVscFv clones. The complementarity-determining regions (CDRs) of the VL (top) and VH (below) fragments are in black-bordered rectangles.

| K9RABV clone | Antibody type | | CDR3 AA sequence | Germline | Family | V-gene |
|---|---|---|---|---|---|---|
| scFv1 | Full scFv ($VHVL_{\kappa}$) | $VL_{\kappa}$: | GQGTHFPWT | IGKV2-10*01 | IGKV2 | *IGKV2-10* |
| | | VH: | AREAYMGLYNFDY | IGHV3-5*01 | IGHV3 | *IGHV3-5* |
| scFv2 | Full scFv ($VHVL_{\kappa}$) | $VL_{\kappa}$: | GQGTHDPWT | IGKV2-5*02 | IGKV2 | *IGKV2-5* |
| | | VH: | AASIEY | IGHV3-5*01 | IGHV3 | *IGHV3-5* |
| scFv12 | Full scFv ($VHVL_{\kappa}$) | $VL_{\kappa}$: | GQGIQDPPGT | IGKV2-6*01<br>IGKV2-9*01 | IGKV2 | *IGKV2-6*<br>*IGKV2-9* |
| | | VH: | GDSWPLDS | IGHV3-5*01 | IGHV3 | *IGHV3-5* |
| scFv15 | Full scFv ($VHVL_{\lambda}$) | $VL_{\lambda}$: | GQNLQFPYT | IGLV2-5*02 | IGLV2 | *IGLV2-5* |
| | | VH: | ANHPYPVATDPFDH | IGHV3-6*01 | IGHV3 | *IGHV3-6* |
| scFv16 | Full scFv ($VHVL_{\kappa}$) | $VL_{\kappa}$: | GQGVQFPRT | IGKV2-5*02 | IGKV2 | *IGKV2-5* |
| | | VH: | ARDVNYYISDY | IGHV3-41*01 | IGHV3 | *IGHV3-41* |

**Table 1**. Sequence diversity of the five selected K9RABVscFv fragments compared with the ig germline IMGT database.

neutralization activity, whereas K9RABVscFv2, 12, and 15 did not inhibit CVS-11 (Table 2). The neutralizing titers of K9RABVscFv1_1 and K9RABVscFv1_2 were 3.51 and 4.96 IU/ml, respectively, whereas those of K9RABVscFv16_1 and K9RABVscFv16_2 were 2.37 and 5.65 IU/ml, respectively. Moreover, these 4 purified scFv samples presented neutralizing titers greater than the protective level of 0.5 IU/ml.

Notably, both neutralizing scFv concentrations were approximately 5 mg/ml, and the RVNA titers of K9RABVscFv1 and K9RABVscFv16 were 3.51 IU/ml and 2.37 IU/ml, respectively. This means that the neutralization ability of K9RABVscFv1 is slightly better than that of K9RABVscFv16, as described in Fig. 10. Notably, dose-dependent effects on RVNA titers were detected when the concentrations of both antibodies were increased to approximately 7 mg/ml. However, the neutralizing potencies of these two clones at a concentration of 7 mg/ml were contrary to the results at a concentration of 5 mg/ml.

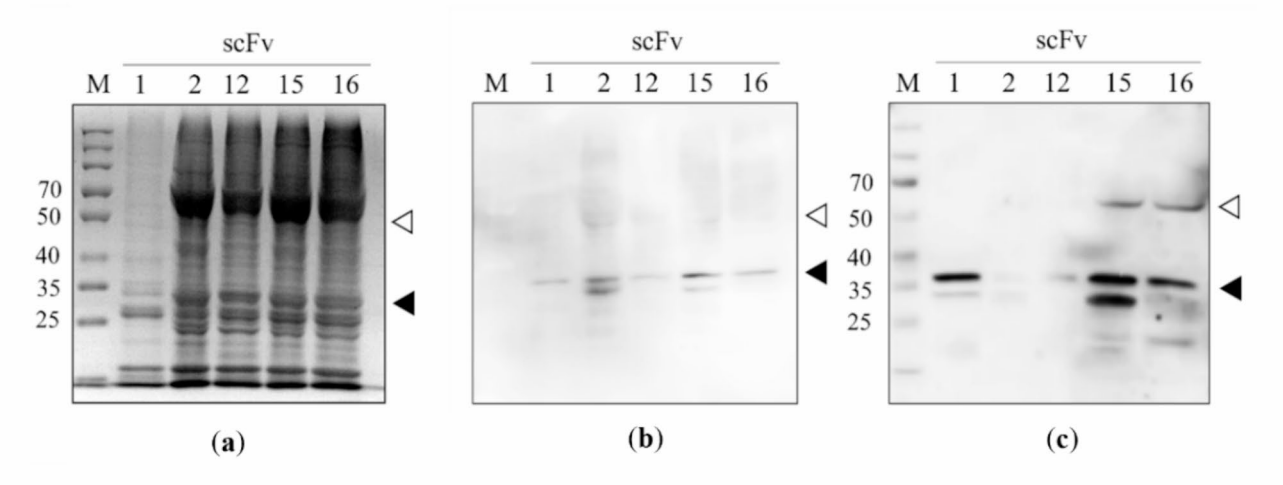


**Fig. 8**. SDS-PAGE and Western blot analysis of the five purified, concentrated, and soluble K9RABVscFv clones. The actual scFv molecular weight was approximately 30–37 kDa (black arrow), and a 60-kDa (white arrow) dimeric form of scFv was observed in four clones. (**a**) SDS-PAGE analysis of 5 K9RABVscFv (**b**) Anti-6XHIS tag-conjugated HRP secondary monoclonal antibody (clone HIS-1, Sigma-Aldrich, UK) at a concentration of 1:10,000 bound to the scFv antibody in the WB assay and detected by ECL reagents (Cytiva Amersham). (**c**) All five scFv antibodies incorporated with primary antibody 1:5,000 dilution of unconjugated goat anti-human IgG [$F(ab')_2$] (Invitrogen; Thermo Fisher Scientific) and a 1:5,000 dilution of HRP-conjugated rabbit anti-goat IgG (H + L) (Invitrogen; Thermo Fisher Scientific) as a secondary antibody. The secondary antibodies were detected via enhanced chemiluminescence (ECL) reagents (Cytiva Amersham). The original Western blot images are shown in Fig. S3. A Spectra Multicolor Broad Range Protein Ladder (Thermo Scientific) was used in panels (**a**) and (**c**).

## Bioinformatics: K9RABVscFv1 and K9RABVscFv16 homology modeling and molecular docking analysis

*Homology model constructions of K9RABVscFv1, K9RABVscFv16, and RABV-G*

To predict the interaction sites between neutralizing scFv antibodies (K9RABVscFv1 and K9RABVscFv16, the full amino acid sequences are shown in Fig. S2) and the rabies virus glycoprotein (RABV-G; SQ382, Thai-street rabies virus, Fig. S2), bioinformatics was implemented before in vitro epitope mapping. The analysis parameter scores of the homology models are presented in Table S3. The crystal structure of the human stapled scFv (spFv) GLK1 clone (PDBID: 8dy2.1. A, X-ray, 1.65 Å resolution)[24] was selected as an appropriate template for homology modeling and 3D-structural model generation of the K9RABVscFv1 antibody, whereas the crystal structure of the 4M5.3 anti-fluorescein human scFv (PDBID: 1 × 9q, X-ray, 1.5 Å resolution)[25] was used as a template for K9RABVscFv16. In the case of RABV-G (SQ382, 524 amino acids) homology modeling, the monomer form of the prefusion RABV-G trimers PDBID no. 7u9g (electron microscope, 3.39 Å resolution)[4] was the best template.

The tertiary structural graphics of K9RABVscFv1, K9RABVscFv16, and RABV-G (SQ382) are shown in Fig. 11. Notably, all the predicted CDRs were located on the outer loop of the VL and VH chains. Previously reported antigenic sites on RABV-G[26,27] were indicated as colorful clusters on the ectodomain of RABV-G.

## In silico molecular docking of neutralizing scFv clones and RABV-G

The best prediction models for the K9RABVscFv1 vs. RABV-G (SQ382) and K9RABVscFv16 vs. RABV-G (SQ382) complexes were selected on the basis of the smallest HADDOCK scores, which were $-100.8 \pm 6.4$ and $-79.5 \pm 3.9$, respectively. The root mean square deviations of K9RABV scFv1 and K9RABVscFv16 were $0.5 \pm 0.3$ °A and $0.4 \pm 0.4$ °A, respectively. The most likely binding conformation between the CDR1-3 area on K9RABVscFv1 and the antigenic sites on RABV-G is shown in Fig. 12, and the K9RABVscFv16-bound RABV-G complex is shown in Fig. 13.

The analysis also revealed the binding sites on scFv (CDR1, 2, 3 and FR1, 2, 3 of VL and VH) and RABV-G (antigenic sites I, IIa, IIb, III, IV, and a), which were determined from the positions of amino acid residues. The interactions between the residues on the CDR of the scFv and the antigenic sites on RABV-G are shown in Table 3.

Computational predictions of binding between K9RABVscFv1 and the RABV-G complex revealed that residues on antigenic sites IIa, IIb, and III together with CDR-1 and CDR-3 of the VL chain and CDR-1, CDR-2, and CDR-3 of the VH chain are involved in these interactions. The 18 binding sites showed interactions between residues on CDRs and antigenic sites, but two residues on scFv (Q24 and E226) recognized the same residues on RABV-G (R352 and K217, respectively), with different types of hydrogen bonds and ion pairs. Overall, 100% of the residues on epitope III significantly interacted with residues on the CDR of the VL chain, especially R352 on epitope III of RABV-G, which could bind to several sites on the CDR of VL. All residues on antigenic site IIa interact with residues on the CDR of the VH chain. Residues on epitope IIb interact with residues on the CDR

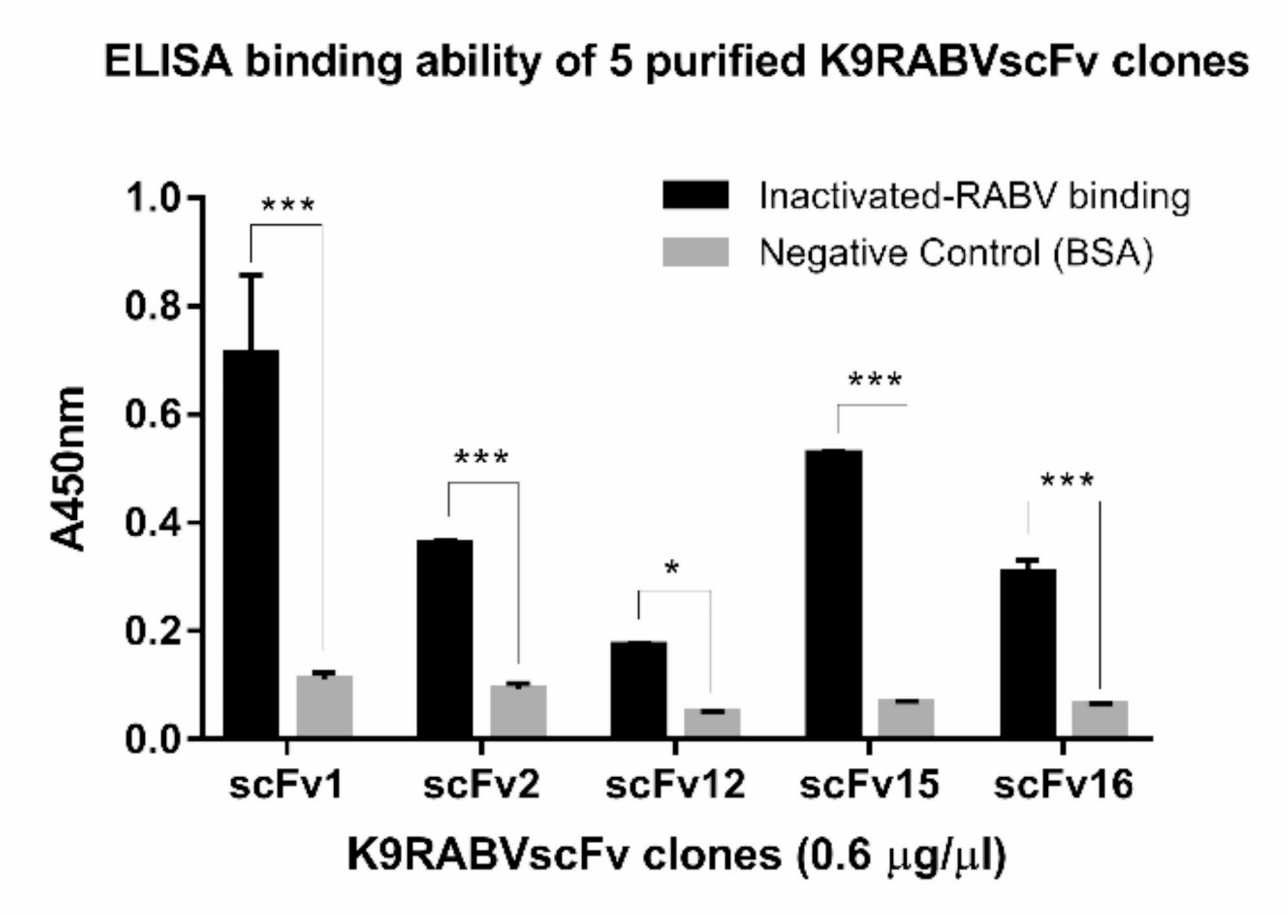


**Fig. 9**. ELISA binding absorbance signal at 450 nm of five purified soluble K9RABVscFv clones (0.6 μg/μl; total 60 μg/well). BSA was used as a negative control. Asterisks indicate significant differences at $P$ values ≤ 0.05 (*), ≤ 0.01 (**), and ≤ 0.001 (***). A TMB substrate was used for detection. The error bars indicate the SDs of duplicate samples.

| scFv | Concentration (mg/ml) | Neutralizing activity | RFFIT Titer (IU/ml) | > Cutoff value at 0.5 IU/ml |
|---|---|---|---|---|
| K9RABVscFv1_1<br>K9RABVscFv1_2* | 5.35<br>7.35 | Positive<br>Positive | 3.51<br>4.96 | ✓<br>✓ |
| K9RABVscFv2 | 6.12 | Negative | - | – |
| K9RABVscFv12 | 4.08 | Negative | - | – |
| K9RABVscFv15 | 4.30 | Negative | - | – |
| K9RABVscFv16_1<br>K9RABVscFv16_2* | 5.88<br>7.11 | Positive<br>Positive | 2.37<br>5.65 | ✓<br>✓ |
| Control | Concentration (mg/ml) | Neutralizing activity | RFFIT Titer (IU/ml) | > Cutoff value at 0.5 IU/ml |
| 1 IU RAI | 6.7 | Positive | 1 | ✓ |
| ERIG 1<br>ERIG 2 | 0.17<br>1.70 | Positive<br>Positive | 1<br>10 | ✓<br>✓ |
| Negative control | – | Negative | 0 | – |

**Table 2**. The RFFIT neutralizing activity of seven purified K9RABVscFv samples. A total of 8 fields per well were observed. Only negative fields were counted. RAI = Human rabies immunoglobulins (reference standard). ERIG = TRCS® Equine Rabies Immunoglobulins (as an internal control). Negative control = serum from healthy, RABV-unvaccinated individuals.

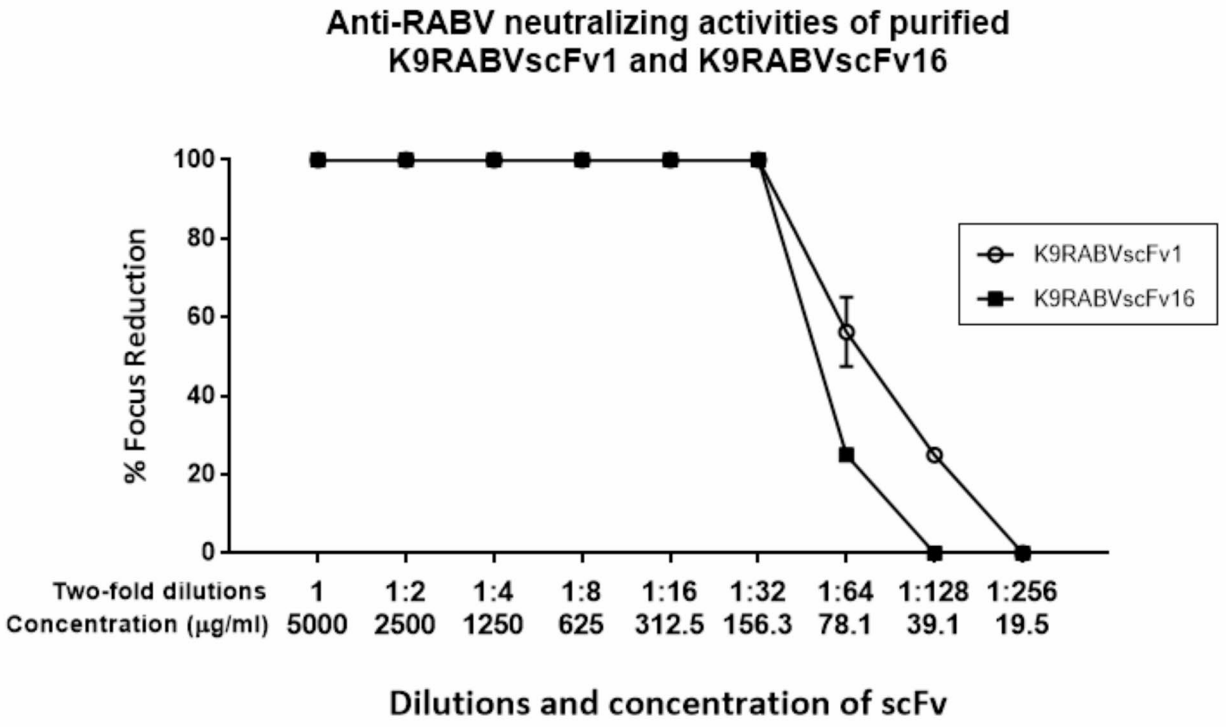


**Fig. 10**. Percent neutralization of K9RABVscFv1 (5.35 mg/ml) and K9RABVscFv16 (5.88 mg/ml) interpreted from the RFFIT results. Twofold dilutions of both antibodies were conducted from 1:2 to 1:256. A total of 8 fields per well were observed. Percent neutralization was calculated from the number of negative fields.

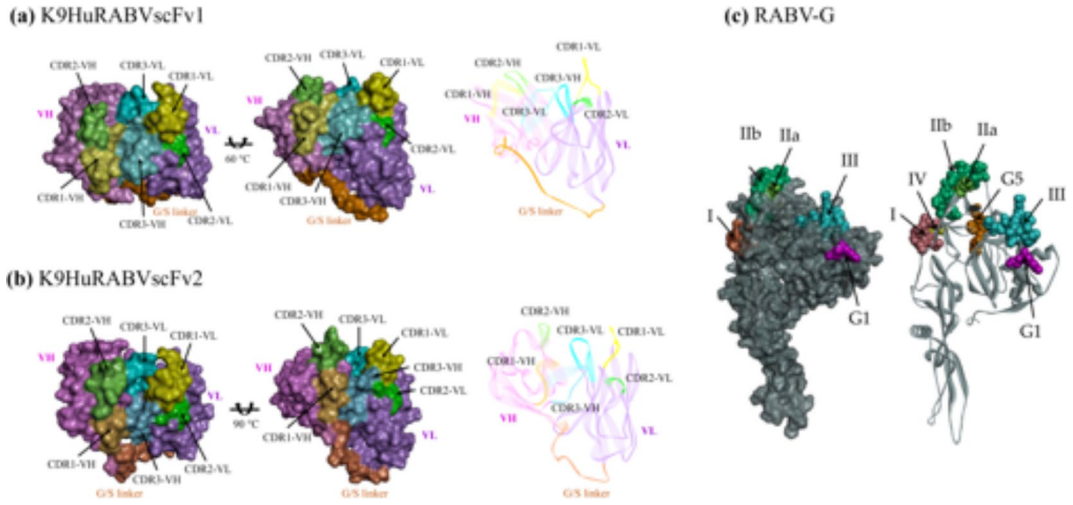


**Fig. 11**. Three-dimensional (3D) tertiary structure prediction of the K9RABVscFv1 and K9RABVscFv16 antibodies and the rabies virus glycoprotein (RABV-G). PDBID no. 1×9q, 8dy2.1. A and the monomer form of PDBID no. 7u9g were used as templates for K9RABVscFv1, K9RABVscFv16, and RABV-G protein structure simulations. The light purple and pink clusters represent the VL and VH chains, respectively. The orange fragment was a glycine/serine linker (G/S linker). CDR1–3 on the VH and VL chains are shown in several colors. Surface display and line-ribbon style of (**a**) K9RABVscFv1, (**b**) K9RABVscFv16, and (**c**) RABV-G (SQ382). The SWISS model online server (https://swissmodel.expasy.org/) was used to construct protein structure homology models, which were decorated with BIOVIA Discovery Studio Visualizer 2021.

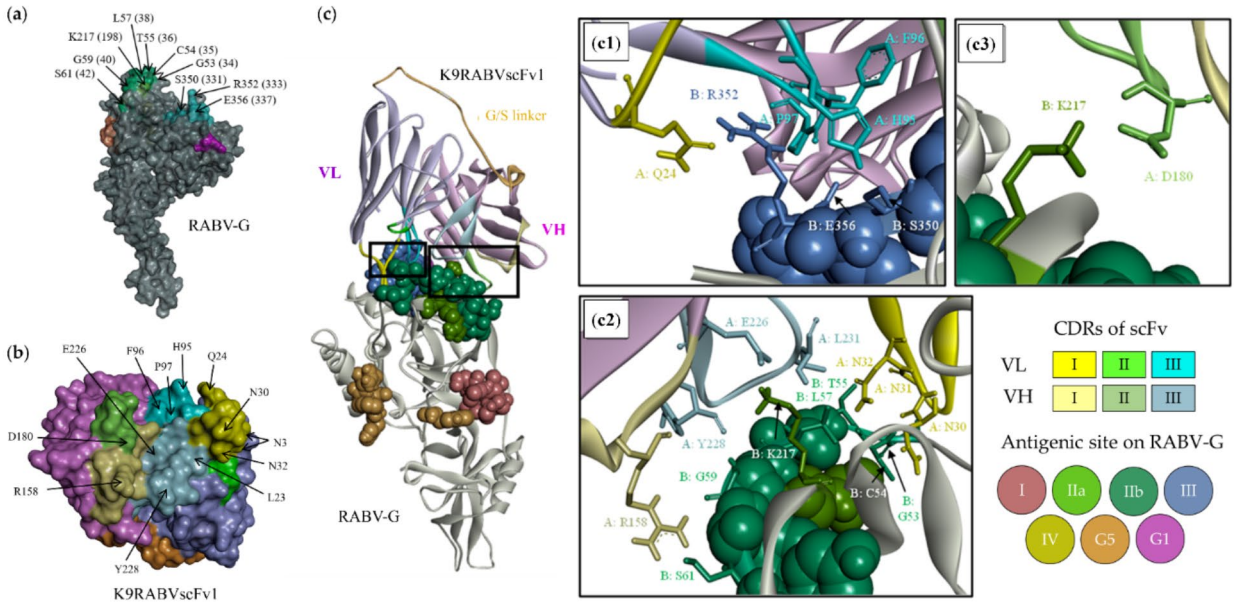


**Fig. 12**. The most likely binding conformation between the CDR1–3 area on K9RABVscFv1 and the antigenic sites on RABV-G was predicted by the HADDOCK 2.4 web server. (**a**) Surface display structures of RABV-G with residues on antigenic sites that interact with (**b**) residues on the CDR of K9RABVscFv1. The numbers in brackets "()" in the RABV-G labels refer to the positions without 19 amino acids in the signal sequence. (**c**) Interactions between the residues on the CDR of K9RABVscFv1 and the antigenic sites of RABV-G on the basis of the results in Table 3. The sticks display the amino acid residues on the CDR (chain A) that interact with the residues on the antigenic sites of RABV-G (chain B). Significant interactions are shown in panels (**c1**), (**c2**), and (**c3**). The VH chain, VL chain, G/S linker, CDR1–3 VH, CDR1–3 VL, antigenic major sites I, II, III, IV, and G5, and minor site G1 (or "a") are shown in different colors.

of the VL or VH chain. The 11 residues on the CDRs of VL, CDR1-VL (6/18), and CDR3-VL (5/18) recognized residues on RABV-G epitopes IIb (4/18) and III (7/18), whereas the seven residues on the CDRs of VH, CDR1-VH (2/18), CDR2-VH (1/18), and CDR3-VH (4/18) interacted with epitopes IIa (3/18) and IIb (4/18).

K9RABVscFv16 also interacted with RABV-G, particularly residues at antigenic sites IIa, IIb, and III, together with the CDR-1 of VL and CDR-1, -2, and − 3 of the VH chain. Twelve binding sites showed interactions between residues on the CDR and antigenic sites; the binding residues on the CDR were predominantly located on the CDRs of VH (9/12), consisting of CDR1-VH (4/12), CDR2-VH (1/12), and CDR3-VH (4/12). Almost all of them possibly bind to epitope II, which is divided into IIb (7/12) and IIa (2/12), whereas only three residues of CDR1-VL may bind to antigenic sites on RABV-G, especially epitope III (3/12). Docking prediction indicated that S158 on scFv could bind to two residues of epitope II, L57 (IIb) and K217 (IIa).

## Discussion

Rabies is a fatal infectious disease in mammals that can be transmitted to humans. A recent report in Thailand revealed that pet dogs are most affected, especially those that are unvaccinated and roam freely or semifreely[1]. Passive immunotherapy products such as monoclonal antibodies (MAbs) have been developed to combat rabies in humans but not domestic animals[17–23,28]. For example, the World Health Organization (WHO) established a postexposure prophylaxis (PEP) category III protocol using antibodies against rabies virus for human patients who come in contact with suspected rabid animals[10,29]. According to WHO guidelines, a rabies virus RFFIT neutralizing antibody (nAb) level greater than or equal to 0.5 IU/ml is associated with an adequate response (seroconversion) to a complete vaccination program[10,29–31]. Interestingly, Bunn and Ridpath (1984) previously reported an association between a minimum titer of 0.5 IU/ml and a protective level from the challenge study in dogs, confirming seroconversion in humans[32]. The statistical analysis of prechallenge titers and survival rates revealed that the titers were approximately 0.2 and 0.5 IU/ml, resulting in 95% and 99.99% survival rates, respectively. Moreover, with respect to the WHO and FDA guidance for therapeutic anti-RABV MAb development, they recommend the use of anti-RABV MAb cocktails as an alternative passive immunity to rabies immunoglobulin (RIG) in rabies postexposure prophylaxis (PEP). These neutralizing MAbs should bind to nonoverlapping epitopes of the RABV glycoprotein and have activity against a diverse panel of rabies virus strains[33,34]. Thus, a large diversity in the complementarity-determining regions (CDRs) of antibodies is needed because we have a greater probability of discovering neutralizing clones that can bind to different epitopes and against viruses. This study used pComb3XSS phage display to generate canine scFv (MAbs) as a passive immunotherapy for animals exposed to rabies.

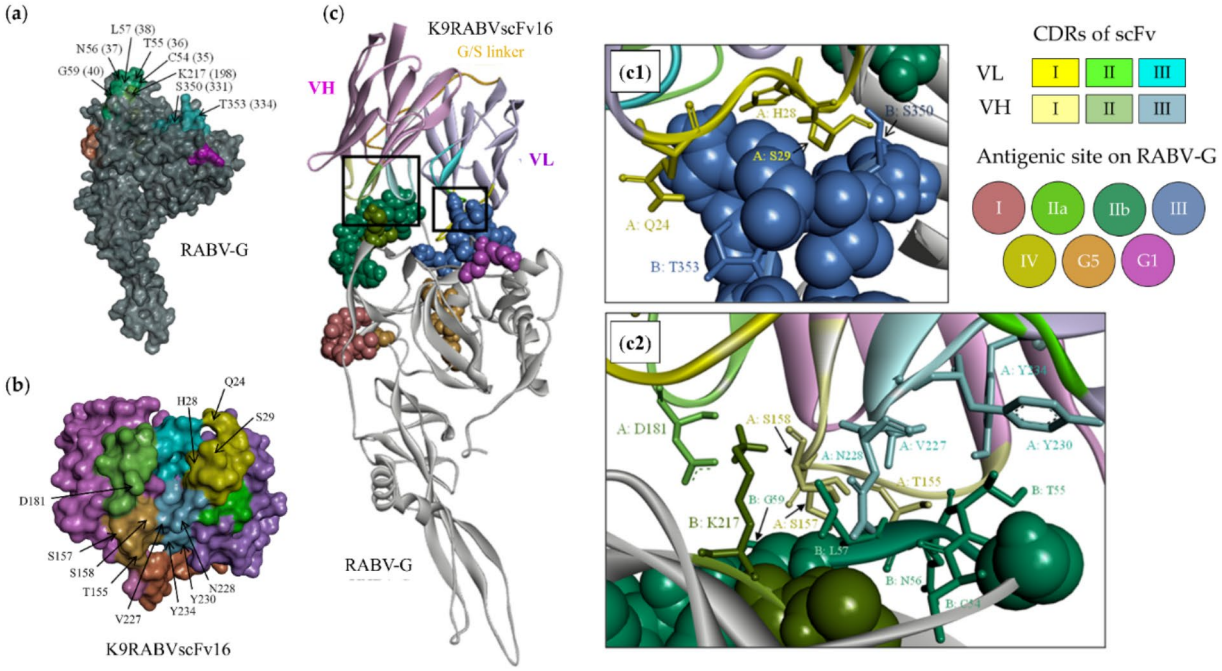


**Fig. 13**. The most likely binding conformation between the CDR1–3 area on K9RABVscFv16 and the antigenic sites on RABV-G was predicted by the HADDOCK 2.4 web server. (**a**) Surface display structures of RABV-G with residues on antigenic sites that interact with (**b**) residues on the CDR of K9RABVscFv1. The numbers in brackets "()" in the RABV-G labels refer to the positions without 19 amino acids in the signal sequence. (**c**) Interactions between the residues on the CDR of K9RABVscFv1 and the antigenic sites of RABV-G on the basis of the results in Table 3. The sticks display the amino acid residues on the CDR (A chain) that interact with the residues on the antigenic sites of RABV-G (B chain). Significant interactions are shown in panels (**c1**) and (**c2**). The VH chain, VL chain, G/S linker, CDR1–3 VH, CDR1–3 VL, antigenic major sites I, II, III, IV, and G5, and minor site G1 (or "a") are shown in different colors.

Here, scFv libraries were constructed from pooled PBMCs of rabies-vaccinated dogs. In vivo immunized blood samples were collected from 13 healthy mixedbred dogs. All donors were hyperimmunized with rabies, and increases in antirabies antibody titers were monitored every vaccination. Whole blood samples (10 mL) from individual dogs were collected within 14 to 21 days after each vaccination. During this period, activated B cells within the germinal center differentiate into plasma cells that secrete antirabies antibodies into the bloodstream. This significantly increased the levels of individual RFFIT serum neutralizing antibodies. The overall titer was 20–30 IU/ml, which is greater than the WHO's minimum protective level[10,35].

Several phagemid systems have been harnessed to construct phage display scFv libraries[36–40]. We used the pComb3XSS phagemid system in this work. Modified primer sets for pComb3XSS based on Braganza et al.. (2011)[41] were used to generate canine scFv antibody libraries in the VL-linker-VH platform. Although phage display-related PCR amplification of the VH and VL genes for scFv or Fab antibodies of species-specific immunoglobulin repertoires has been reported[38,42–51], few phage display systems and PCR protocols have been developed for canine antibody libraries.

Braganza and colleagues designed and validated sets of degenerate primers specific to canine IgG and IgM repertoires on the basis of the diverse rearrangements of antibody variable genes in both the heavy and light chains. To access the entire canine antibody gene, all possible products of forward and reverse primers for VH and VL were amplified via 65 independent PCRs. The flexible glycine-serine linker enables the random assembly of diverse VL and VH fragments via pull-through overlapping extension PCR assays. However, we modified some nucleotide bases on the CSCG1234-B and RSC-B primers to be complementary to the DNA template correctly.

This study created two diverse phage-displayed canine scFv libraries against the rabies virus due to different isotypes of the VL chain, such as the VLκ-VH and VLλ-VH libraries, as described in previous publications[41,52]. The VLκ-VH and VLλ-VH libraries contained $2.4\times10^8$ and $1.3\times10^6$ clones, respectively. Approximately $10^6$–$10^9$ transformants in immunized scFv or Fab libraries are sufficient to obtain antibody clones with high affinity for the rabies virus[18,28,37,39,53–56] and other infectious diseases[38,41,52,57,58]. Furthermore, the diversities of these 2 constructed scFv libraries are essentially described by B*stN*I fingerprint techniques, which are common, easy, and inexpensive methods for screening the different patterns of antibodies in phage display libraries[37,38,41,59–61]. Interestingly, the VHVLλ library shows 100% complete unique patterns of overall clones (15/15), whereas 93.33% (unique 14 patterns out of 15 clones) of the randomized clones of the VHVLκ library vary.

| Docking group | ΔG (kcal/mol) | Kd (M) At 25 °C | scFv | | | RABV-G | | | Interaction bond or force |
|---|---|---|---|---|---|---|---|---|---|
| | | | CDR | sequence | Residue* | Antigenic site | sequence | Residue* | |
| K9RABVscFv1 VS RABV-G | -12.6 | $6.2\times10^{-10}$ | CDR2-VH | TS**D**SGSST | D180 | IIa | **K**RA | K198 | Electrostatic |
| | | | CDR3-VH | AR**E**AYMGLYNFDY | E226 | | **K**RA | K198 | Hydrogen bond |
| | | | CDR1-VL | QSLLHS**N**GNTY | N30 | IIb | **G**CTNLSGFSY | G34 | Hydrogen bond |
| | | | CDR1-VL | QSLLHS**N**GNTY | N30 | | G**C**TNLSGFSY | C35 | Hydrogen bond |
| | | | CDR1-VL | QSLLHSNG**N**TY | N32 | | G**C**TNLSGFSY | C35 | Hydrogen bond |
| | | | CDR1-VL | QSLLHSNG**N**TY | N32 | | GC**T**NLSGFSY | T36 | Hydrogen bond |
| | | | CDR1-VH | GFTFS**R**YK | R158 | | GCTNLS**G**FSY | G40 | Hydrogen bond |
| | | | CDR1-VH | GFTFS**R**YK | R158 | | GCTNLSGF**S**Y | S42 | Hydrogen bond |
| | | | CDR3-VH | AREA**Y**MGLYNFDY | Y228 | | GCTNLS**G**FSY | G40 | Hydrogen bond |
| | | | CDR3-VH | AREAYMG**L**YNFDY | L231 | | GCTN**L**SGFSY | L38 | Hydrophobic force |
| | | | CDR1-VL | **Q**SLLHSNGNTY | Q24 | III | KSV**R**TWNEI | R333 | Hydrogen bond |
| | | | CDR3-VL | GQGT**H**FPWT | H95 | | K**S**VRTWNEI | S331 | Hydrogen bond |
| | | | CDR3-VL | GQGT**H**FPWT | H95 | | KSV**R**TWNEI | R333 | Hydrophobic force |
| | | | CDR3-VL | GQGTH**F**PWT | F96 | | KSV**R**TWNEI | R333 | Hydrogen bond |
| | | | CDR3-VL | GQGTHF**P**WT | P97 | | KSV**R**TWNEI | R333 | Hydrogen bond |
| | | | CDR3-VL | GQGTHF**P**WT | P97 | | K**S**VRTWN**E**I | E337 | Hydrogen bond |
| K9RABVscFv16 VS RABV-G | -11.6 | $2.9\times10^{-9}$ | CDR1-VH | GFTFS**S**YH | S158 | IIa | **K**RA | K198 | Hydrogen bond |
| | | | CDR2-VH | IRF**D**GSYP | D181 | | **K**RA | K198 | Hydrogen bond |
| | | | CDR1-VH | GF**T**FSSYH | T155 | IIb | GCT**N**LSGFSY | N37 | Hydrogen bond |
| | | | CDR1-VH | GFTFS**S**YH | S157 | | GCTNLS**G**FSY | G40 | Hydrogen bond |
| | | | CDR1-VH | GFTFS**S**YH | S158 | | GCTN**L**SGFSY | L38 | Hydrogen bond |
| | | | CDR3-VH | ARD**V**NYYISDY | V227 | | GCTN**L**SGFSY | L38 | Hydrophobic force |
| | | | CDR3-VH | ARDV**N**YYISDY | N228 | | G**C**TNLSGFSY | C35 | Hydrogen bond |
| | | | CDR3-VH | ARDVNY**Y**ISDY | Y230 | | GCTNLSGFSY | T36 | Hydrophobic force |
| | | | CDR3-VH | ARDVNYYISD**Y** | Y234 | | GCTNLSGFSY | T36 | Hydrogen bond |
| | | | CDR1-VL | **Q**SLLHSNGNTY | Q24 | III | KSVR**T**WNEI | T334 | Hydrogen bond |
| | | | CDR1-VL | QSLL**H**SNGNTY | H28 | | K**S**VRTWNEI | S331 | Hydrogen bond |
| | | | CDR1-VL | QSLLH**S**NGNTY | S29 | | K**S**VRTWNEI | S331 | Hydrogen bond |

**Table 3**. Summary of the docking results for the CDRs of K9RABVscFv and the antigenic sites on RABV-G. * The amino acid positions exclude the first 19 amino acids of the signal sequence. Bold-highlighted letters in the sequences refer to residues that showed the interaction.

We used inactivated RABV and recombinant RABV-G in their native trimeric and monomeric conformations as antigens for affinity selection. Compared with the common affinity selection method, including a subtraction step significantly increased the output titer in each panning round of either inactivated whole RAVB or recombinant RABV-G binding (data not shown). However, the bound phage titers of the second round were generally lower than the outputs of the first round in all the selection groups because of the selection of higher-affinity binding clones. After selection, an estimated 10-fold enrichment of high-affinity bound phage clones was observed in subsequent rounds.

The diversity of CDRs on the VL and VH sequences of binding affinity scFv clones can be characterized from their DNA and protein sequences after selection. Conventional Sanger sequencing can reveal the variety of nucleotide bases and amino acid arrangements of individually randomized clones[18,37,39,54,55,57,60–63]. Here, DNA sequencing of 20 positive ELISA canine scFv clones specific to the rabies virus glycoprotein revealed nine unique pairing patterns on the CDR-1, -2, and −3 sequences of the VH and VL chains, which we call the K9RABVscFv1–9 clones. To further optimize protection against the rabies virus, we performed the RFFIT assay on nine unpurified soluble scFv antibodies prior to scFv protein expression and purification. Finally, the top five high-titer K9RABVscFv clones consisting of K9RABVscFv1–5 were selected.

Many factors can contribute to the abundance of the selected population. Notably, differences in library diversity might affect the success of repertoire selection. Larger library sizes indicate the possibility of retrieving diverse high-affinity clones[64]. In this study, the VH-VLκ library was 100 times larger than the VH-VLλ library; thus, kappa populations could be selected predominantly. However, another crucial reason was observed in Fig. 3. The colony PCR of the prepanning libraries (16 clones/library) demonstrated that the cloning efficiency of the VH-VLλ library was 75%, whereas 100% cloning efficiency was found for the VH-VLκ library. 25% failure of the VH-VLλ library resulted in an incomplete scFv with a size of approximately 300–600 bp, whereas perfect 800–900 bp sizes of scFv from the VH-VLκ library were observed. In addition to the difference in library size between them, the reduction in complete VH-VLλ clones in the library might cause a decline in the lambda light chain populations after selection compared with the kappa light chain.

The results of the purified-scFv ELISA (Fig. 9) revealed that the binding ability of K9RABVscFv15 was much greater than that of K9RABVscFv16, but it did not exhibit RFFIT-neutralizing activity. K9RABVscFv15 might be categorized as a nonneutralizing antibody in which CDRs are able to strongly bind with area(s) outside those epitopes or whose CDRs probably bind only a small number of epitopes on glycoproteins and are not tightly bound. The HADDOCK in silico prediction of interactions between K9RABVscFv15 and the RABV glycoprotein basically supported this hypothesis; there were only two interactions between the CDRs of the antibody and antigenic sites among the 15 total interactions (Table S6). In contrast, the neutralizing clones K9RABVscFv1 and K9RABVscFv16 presented approximately twelve CDR-epitope interactions (Tables S4 and S5).

The mechanisms of canine VH and VL diversification are similar to those in humans and mice[65]. Diversity in the variable chain of the antibody arises through somatic recombination of the highly polymorphic VDJ gene of the heavy chain and VJ genes of the light chain, which are located in the CDR3 of the antibody molecule. CDR3 thus provides an "identity tag" that, when coupled with VDJ genes, can be used to identify clonally related sequences derived from the same B-cell precursor[66]. V segment rearrangements of the CDR3 VH and VL chains were determined in V-alleles, genes, and families according to the IMGT alignment of five K9RABVscFv clones from 13 rabies-vaccinated dogs.

The canine IGHV3 and IGKV2 families were predominantly found among the five K9RABVscFv clones. The most preferential V alleles and gene segments of the VH chain were the *IGHV3-5*01* alleles (IGHV3-5 gene), followed by the *IGHV3-6*01* and *IGHV3-41*01* alleles. The most common V alleles and gene segments of VLκ are *IGKV2-5*02* alleles (IGKV2-5 gene), followed by *IGKV2-6*01* alleles (IGKV2-6 gene), *IGKV2-9*01* alleles (IGKV2-9 gene), and *IGKV2-10*01* alleles (IGKV2-10 gene). Research on canine immunoglobulin repertoires and diversity based on V(D)J rearrangement is limited, especially in cases of viral infection and vaccination. One study explored canine B-cell receptor repertoires in 25 healthy dogs of various breeds and 18 dogs with B-cell lymphoma via an NGS assay and bioinformatics[67]. The distribution of the most frequent family used among the V segment of the healthy VH repertoire, the canine IGHV3 family, remarkably accounts for 79.1%, as does another study of the IgG and IgM repertoires of healthy different dog breeds; the use of the IGHV3 family accounts for more than 90% of the IgG repertoire and 91–98% of the IgM repertoire[68]. The commonly used V-gene segments of the variable heavy chain, *IGHV3-41* and *IGHV3-5*, are reported in greater than 11% and 7% of rearrangements, respectively, in healthy dogs. However, *IGHV3-38* is the most commonly used gene in dogs with and without lymphoma among all V gene segments of VH, accounting for more than 26% of the V gene segment in the healthy group. *IGHV3-6* comprised less than 5% of the total genes. In the V segment of the VLκ chain, the *IGKV2* family composes 99.7% of the V segment. *IGKV2-5* was found in 20.3% of the cases, whereas *IGKV2-6*, *IGKV2-9*, and *IGKV2-10* accounted for less than 5%. For the V segment of the VLλ chain, only 0.8% of the IGLV2 family is used[67]. In addition, combinations of IGHV3- and IGKV2-germline families were found in all the K9RABVscFv clones except K9RABVscFv15, in which the IGHV3 and IGLV2 families were paired.

Germline mutations were found in the CDR3 amino acid sequences. The nonsilent mutations included M105G and Q109H on CDR3-VL and S106R on CDR3-VH of K9RABVscFv1. The mutations I108T and Q109H were found in the CDR3-VL chain of K9RABVscFv2, whereas the mutation S106A was found in CDR3-VH. For K9RABVscFv12, only the VH chain presented the amino acid changes A105G and S106D on CDR3, with no mutations in VL. G107N, I108, and D110F were discovered in the CDR3 of the VL of K9RABVscFv15, whereas silent and nonsilent mutations disappeared in the CDR3 of the VH chain. Finally, K9RABVscFv16 had the nonsilent mutations I108V and D110F on CDR3-VL and K106R on CDR3 of the VH fragment.

In this study, dimerization was observed for all the scFv antibodies. The dimer–monomer equilibrium normally depends on many factors, such as linker length, antibody sequence, and environmental conditions[69]. Previous studies have shown that repetitive GS linkers longer than 12 or 15 residues should allow the proper orientation of the VH and VL domains, which are covalently linked variable fragments that form a functional scFv. These are supposed to be monomeric forms rather than oligomeric forms by binding with other scFv molecule(s), whereas linkers shorter than 12 or 15 usually have multimeric forms[70–72]. Therefore, the length of linkers that we applied in this study (18 amino acids) might not be the main cause of dimerization. However, the occurrence of the dimeric form can complicate our understanding of the effects of scFv affinity and/or avidity[73,74]. The HisTrap™ immobilized metal affinity chromatography column (Cytiva) was used for polyHis-tagged antibody purification here and in other studies[37,38,57,75]. However, impurities in the eluted scFv fractions are always observed. Using other affinity chromatography columns, such as protein L and cobalt IMAC, can increase the purity of concentrated scFv proteins.

The neutralizing titers of purified K9RABVscFv1 and K9RABVscFv16 exceeded the minimum protective level. On the basis of two purified K9RABVscFv1 clones at different concentrations, a 1.4-fold increase in concentration resulted in a 1.4-fold increase in the RVNA titer, which agrees with a previous pMOD/anti-RABV scFv library study[37,] where a 10-fold increase in the IRA7c scFv concentration (0.5 mg/ml vs. 4.9 mg/ml) resulted in a 10-fold increase in the RVNA titer (2.27 vs. 20.13 IU/ml). However, this did not apply to K9RABVscFv16, for which a 1.2-fold increase in the concentration elicited a 2.4-fold increase in the neutralizing titer. The antibody potency of the K9RABVscFv1 clone was slightly greater than that of K9RABVscFv16 at a scFv concentration of approximately 5 mg/ml, in contrast to the results at a concentration of 7 mg/ml.

Bioinformatics-based interaction predictions revealed that some residues on the CDRs of K9RABVscFv1 and K9RABVscFv16 possibly bind to the amino acids on the antigenic sites of RABV-G. Few studies have mapped the epitopes of canine anti-RABV monoclonal antibodies (MAbs) on RABV-G. Most RABV-G antigenic sites have been identified for mouse and human antibodies. Here, 3D-computational predictions revealed that either K9RABVscFv1 or K9RABVscFv16 probably recognizes antigenic sites II and III of RABV-G. The residues on the CDRs of both scFv clones predominantly interact with the residues on antigenic site IIb, followed by binding to site III and minor recognition of site IIa. Notably, the CDRs of K9RABVscFv1 interacted more with epitopes IIb and III than the other clones did. Similar to previous findings, the mouse MAb M777-16-3 can bind to antigenic

site IIa[76]. Human MAbs 11B6, A11, RV01, RV03, RV05, RV08, and RV09 [18,40,78] interact with antigenic site IIb, whereas human MAbs HuMab 17C7, CR4098, RV3A5, RVC58, NP-19-9, and humanized MAb CTB011 bind to antigenic site III of RABV-G[77–82].

Binding affinity prediction: Furthermore, we used PRODIGY to predict the binding affinity in terms of ΔG and Kd. PRODIGY is a reliable biomolecular interaction prediction software used for predicting the binding affinity of protein–protein complexes on the basis of intermolecular interactions. It was developed by Bonvinlab, the same research group as HADDOCK. A lower ΔG thus results in a higher binding affinity; therefore, these two-docking 3D structures are favorable.

The interaction between the antibody and residue K198 on antigenic site IIa (residues 198–200) was also detected via K9RABV scFv1 and 16/RABV-G docking. This is a critical epitope of the MAb M777-16-3 [77]. For antigenic site IIb (residues 34–42), the CDRs of K9RABVscFv1 can interact with the motif "GCT-L-G-SY," whereas the CDRs of K9RABVscFv16 can match the motif "-CTNL-G—." These two neutralizing clones also had different binding motifs to conformational antigenic site III (residues 330–338). The CDRs-VL of K9RABVscFv1 can bind to "-S-R—EI," whereas the CDR1-VL of K9RABVscFv16 interacts with the motif "-S- -T- - - -." R333 was found to be the major binding residue on antigenic site III of RABV-G, followed by S331. Previous studies have shown that residue 333 is polymorphic, unlike S331, which is a conserved region[83]. Moreover, substitutions at position 333 are related to the neutralization and pathogenicity of RABV[7,78,84–86]. To enhance the prediction of epitope binding, we further performed a competitive ELISA between K9RABVscFv1 and K9RABVscFv16. Figure S4 shows that the signals of K9RABVscFv1 and K9RABVscFv16 were significantly different and strongly competitive ($p$ values $\leq 0.05$ and $\leq 0.01$, respectively). These results suggest that the competitive effect of these two clones may be due to the ability of K9RABVscFv1 to bind more strongly than the other strains. However, according to the in silico epitope mapping prediction, either K9RABVscFv1 or K9RABVscFv16 can bind to antigenic site II and some of site III, but some residues that interact with both scFvs at antigenic sites are dissimilar. Hence, it could not be completely concluded that there was no synergistic binding of these two clones because of the binding of K9RABVscFv16 and some interactions of K9RABVscFv1 with RABV. These two K9RABVscFv clones might be engineered and designed with distinct labeled enzymes or detection tags. It is an appropriate procedure to evaluate and clarify the competitive binding of multiple antibodies. Many assays, such as Western blotting, peptide array, alanine scanning, etc., have been used to prove that epitope mapping can localize the binding area with accuracy and reliability. Moreover, the binding affinity of RABV-G should be studied in vitro to confirm and validate the computational predictions.

## Conclusions

In this study, two canine RABV neutralizing monoclonal antibodies, K9RABVscFv1 and K9RABVscFv16, were generated from VL-VH- and VL-VH-immunized pComb3XSS phage display libraries containing $2.4 \times 10^8$ and $1.3 \times 10^6$ transformants, respectively. These purified K9RABVscFv clones presented neutralizing antibody levels above the WHO cutoff value of 0.5 IU/ml. Based on in silico K9RABVscFv-rabies virus glycoprotein docking predictions, these two neutralizing clones predominantly interacted with the residues on antigenic site II, especially IIb, and slightly bound to site III. Thus, K9RABVscFv1 and K9RABVscFv16 are potential candidates for the development of full-form anti-RABV mAbs. These innovations might be applied for novel postexposure treatment protocols in rabies-susceptible dogs, particularly in owned dogs. However, to confirm the antibody binding affinity and epitope mapping, in vitro studies should be performed.

## Methods

*Blood sample preparation, collection, and plasma neutralization activity measurement*

The animal study was approved by the Faculty of Tropical Medicine—the Institutional Animal Care and Use Committee (IACUC)—number FTM-IACUC 008/2022. All procedures were performed in accordance with the ARRIVE guidelines and relevant regulations. Thirteen healthy dogs were immunized with an attenuated rabies vaccine (Rabisin®) in a three-dose vaccination program and received a booster three weeks after the third dose. Serum samples from all dogs were collected before the first-dose immunization (day 0), 21 days after the first dose (day 21), and 21 days after the second dose (day 42) to determine the overall anti-RABV antibody response via an immunoperoxidase monolayer assay (IPMA). Ten milliliters of whole blood from each vaccinated dog were collected once in an EDTA-containing tube after the last booster for 2 weeks. Individual samples were centrifuged at 1,5000 × g for 10 min to separate the plasma and cell layers. Individual plasma samples were sent to the Queen Saovabha Memorial Institute for measuring the neutralizing anti-RABV antibody titer via the rapid fluorescent foci inhibition test (RFFIT).

### PBMC isolation, total RNA extraction, and cDNA synthesis

The PBMCs were isolated via density gradient centrifugation via the Ficoll-Paque PLUS (GE Healthcare, Uppsala, Sweden) method following the manufacturer's protocol. The PBMCs were stored at -80 °C until use. PBMCs from the samples whose neutralizing antibody titers were greater than 0.5 IU/ml were used for further RNA extraction. Total RNA from pooled PBMCs was extracted via TRIzol reagent (Invitrogen Corp., Carlsbad, CA, USA) according to the manufacturer's protocol. To synthesize cDNA from RNA extracts, reverse transcription was performed via oligo dT and superscript III reverse transcriptase (Invitrogen Corp., Carlsbad, CA, USA).

### Variable chain amplification and single-chain variable fragment (scFv) construction

The synthesized cDNA was used as the template for canine variable heavy chain (VH), variable light kappa chain (VLκ), and lambda chain (VLλ) gene amplification via conventional PCR. The entire amplification steps of the antibody genes are described in Fig. 14. The PCR mixture contained nuclease-free water, 100 ng of cDNA, a final concentration of 1X Phusion GC buffer, 200 µM dNTPs, 0.5 µM each primer, and 0.5 U of Phusion High-Fidelity

DNA polymerase (New England Biolabs, Inc.). Mixtures of canine-specific primers were used as described by Braganza et al. (2011)[41]. All primers were designed for the pComb3XSS phagemid. However, the VH reverse primer was adjusted for a few nucleotide bases (Table 4). The PCR cycling conditions were as follows: initial denaturation at 95 °C for 5 min; 35 cycles of denaturation at 95 °C for 30 s, annealing at 56 °C for 30 s, and

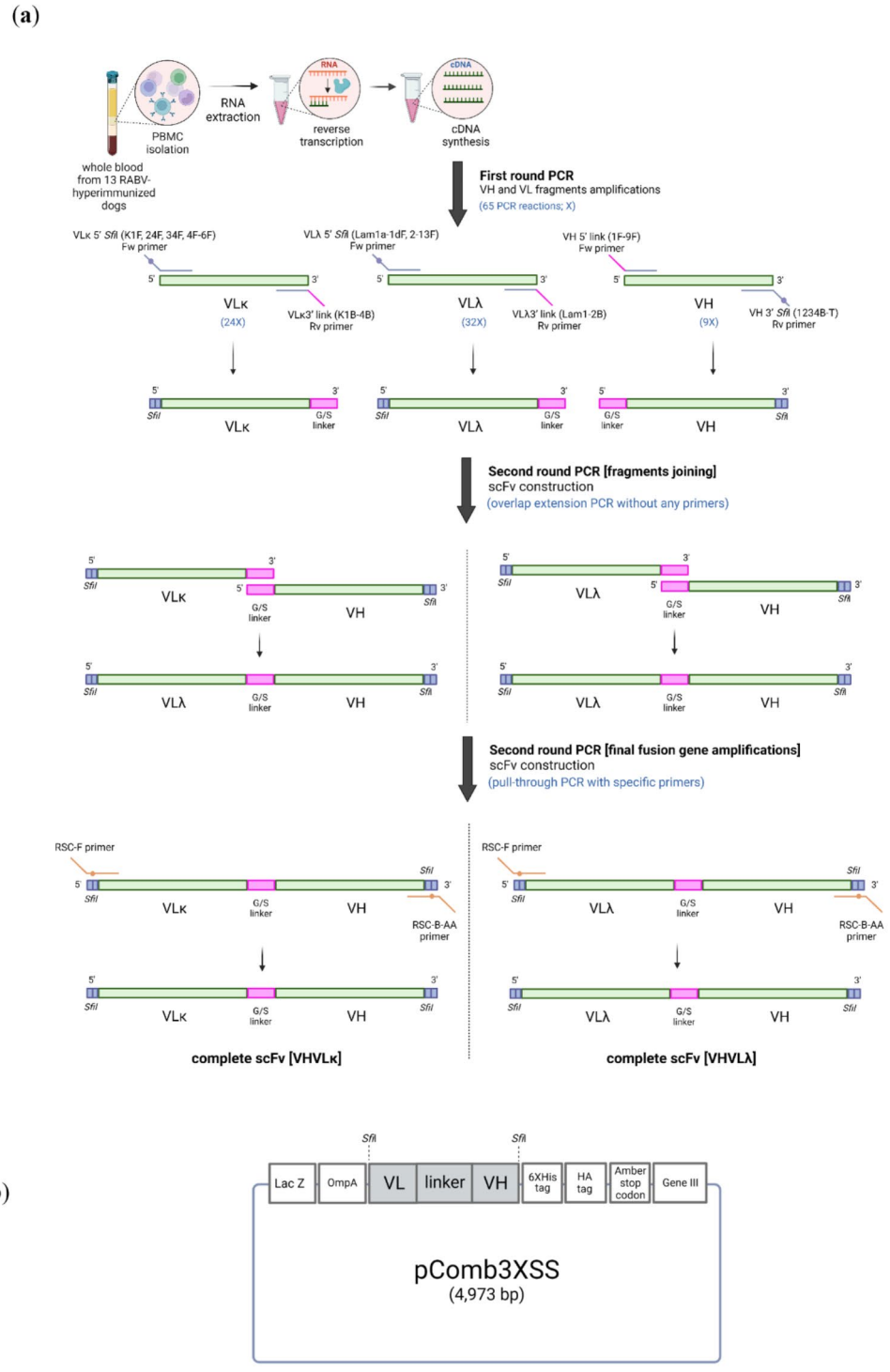


**Fig. 14**. Schematic representation of canine variable-chain fragment amplification and scFv construction via the pComb3XSS phage display system. (**a**) Step of PCR amplification of variable fragments and scFv construction. (**b**) Structure of pComb3XSS harboring the scFv fragment.

| Primer name | Sequence (5'–3') |
|---|---|
| *First round PCR primers* | |
| Canine VH forward primers | |
| CSCVH1-F | GGT GGT TCC TCT AGA TCT TCC TCC TCT GGT GGC GGT GGC TCG GGC GGT GGT GGG GAG GTV CAR CTG GTG SAR TCT |
| CSCVH2-F | GGT GGT TCC TCT AGA TCT TCC TCC TCT GGT GGC GGT GGC TCG GGC GGT GGT GGG GAG GTR MVD YTG GTG GAR TCT |
| CSCVH3-F | GGT GGT TCC TCT AGA TCT TCC TCC TCT GGT GGC GGT GGC TCG GGC GGT GGT GGG GRS GTG CAG CTG GTG GAG TCT |
| CSCVH4-F | GGT GGT TCC TCT AGA TCT TCC TCC TCT GGT GGC GGT GGC TCG GGC GGT GGT GGG GAG GTR CAG CTG STG GAG WMT |
| CSCVH5-F | GGT GGT TCC TCT AGA TCT TCC TCC TCT GGT GGC GGT GGC TCG GGC GGT GGT GGG GAR KWG CAR CTG GTG GAG YTT |
| CSCVH6-F | GGT GGT TCC TCT AGA TCT TCC TCC TCT GGT GGC GGT GGC TCG GGC GGT GGT GGG GAG GGG CAG CTG GCG GAG TCT |
| CSCVH7-F | GGT GGT TCC TCT AGA TCT TCC TCC TCT GGT GGC GGT GGC TCG GGC GGT GGT GGG GAR BTN MAR YTG GTN GAR WSN |
| CSCVH8-F | GGT GGT TCC TCT AGA TCT TCC TCC TCT GGT GGC GGT GGC TCG GGC GGT GGT GGG GAG GTB CAR CTG GTR SAG TCT |
| CSCVH9-F | GGT GGT TCC TCT AGA TCT TCC TCC TCT GGT GGC GGT GGC TCG GGC GGT GGT GGG GAG GTG CAA CTG VWG RAG TCY |
| Canine VH reverse primer | |
| CSCG1234-B-T | CCT GGC CGG CCT GGC CAC TAG **T**AA CCG AGG GGG CCG TGG TGG A |
| Canine $VL_{\lambda}$ forward primers | |
| CSCLam1a-F | GGG CCC AGG CGG CCG AGC TCG TGC TGA MTC MGC YRS SYT CD |
| CSCLam1b-F | GGG CCC AGG CGG CCG AGC TCR YSC TGA CTC ARM MGS CCT CM |
| CSCLam1c-F | GGG CCC AGG CGG CCG AGC TCG TSC TGA CTC AGC YDV CCT CA |
| CSCLam1d-F | GGG CCC AGG CGG CCG AGC TCG YGY TGA CYC ARC YRG CCT CM |
| CSCLam2-F | GGG CCC AGG CGG CCG AGC TCN BVY TGA CKC ARC CDD CCT CR |
| CSCLam3-F | GGG CCC AGG CGG CCG AGC TCG TGC TGW CWC AGC YGC CAT CM |
| CSCLam4-F | GGG CCC AGG CGG CCG AGC TCG TGC TGA CTC AGC CTC CYT C |
| CSCLam5-F | GGG CCC AGG CGG CCG AGC TCG RGY TGA CTC AGC YRC CWT C |
| CSCLam6-F | GGG CCC AGG CGG CCG AGC TCG GGY TGA ATC AGS CTY CCT C |
| CSCLam7-F | GGG CCC AGG CGG CCG AGC TCG TDN TVA CYC ARS MRV CMT CA |
| CSCLam8-F | GGG CCC AGG CGG CCG AGC TCT GCT GAC CCA GAC TCC AAG TG |
| CSCLam9-F | GGG CCC AGG CGG CCG AGC TCK CTG ACC CAG MCT MCA AGT GC |
| CSCLam10-F | GGG CCC AGG CGG CCG AGC TCG TRC TGA CYC ARC CKC CKT CW |
| CSCLam11-F | GGG CCC AGG CGG CCG AGC TCG TRM GSA AYC ARC CKC CKT CW |
| CSCLam12-F | GGG CCC AGG CGG CCG AGC TCC TGC TGA CYC ARC CKG CYT CW |
| CSCLam13-F | GGG CCC AGG CGG CCG AGC TCG TRC TGA AYC ARC CKC CKT CW |
| Canine $VL_{\lambda}$ reverse primers | |
| CSCJLam1-B | GGA AGA TCT AGA GGA ACC ACC GCC GAG GAC GGT CAG STG GGT SCC |
| CSCJLam2-B | GGA AGA TCT AGA GGA ACC ACC ACC WAG GAC GGT SAG YTS GRT TCC |
| Canine $VL_{\kappa}$ forward primers | |
| CSCK1-F | GGG CCC AGG CGG CCG AGC TCC AGA TGA CCC AGT CCC CAA |
| CSCK24-F | GGG CCC AGG CGG CCG AGC TCG TSA TGA YRC AGA CYC CAC |
| CSCK34-F | GGG CCC AGG CGG CCG AGC TCG TGA TGA CMC AGT CTC CAG |
| CSCK4-F | GGG CCC AGG CGG CCG AGC TCA YSM TGA CYC AGT KYC CAG |
| CSCK5-F | GGG CCC AGG CGG CCG AGC TCG TSA TGA YRC AGR CBC CAC |
| CSCK6-F | GGG CCC AGG CGG CCG AGC TCT GTC ATG ACA CAG ACC CCA |
| Canine $VL_{\kappa}$ reverse primers | |
| CSCJK1-B | GGA AGA TCT AGA GGA ACC ACC TTT GAG YTC CAC CTK GGT WCC |
| CSCJK2-B | GGA AGA TCT AGA GGA ACC ACC TTT GAG CTC CTC CTT GGT TCG |
| CSCJK3-B | GGA AGA TCT AGA GGA ACC ACC TTT GAG GTC CAC CTT GGT TCC |
| CSCJK4-B | GGA AGA TCT AGA GGA ACC ACC TTT KAT CTC CAV CTT GGT YCC |
| *Second round PCR primers for scFv construction* | |
| RSC-F | GAG GAG GAG GAG GAG GAG GCG GGG CCC AGG CGG CCG AGC TC |
| RSC-B-AA | GAG GAG GAG GAG GAG GAG CCT GGC CGG CCT GGC CAC TAG **AA** |
| *Sequencing primers* | |
| OmpA | AAG ACA GCT ATC GCG ATT GCA G |
| DpSeq | AGA AGC GTA GTC CGG AAC GTC |

**Table 4**. The set of primers based on the pComb3XSS phagemid for canine VH and VL chains and scFv amplification included sequencing primers according to Braganza et al.. (2011)[36]. Highlights refer to adjusted nucleotide bases in the primers.

extension at 72 °C for 2 min; and a final extension at 72 °C for 10 min. The PCR product size was determined via gel electrophoresis.

Three microliters of the first PCR was used as a template for the second reaction. All the same amounts of reagents used in the first reaction were added to a new master mix together with 0.5 µM specific primers (RSC-F/RSC-B-AA) and used for canine scFv amplification. The RSC primers were annealed to conserved recognition sites at the 5′ ends of VH and 3′ ends of VL (Table 4). The conditions for all PCRs were as follows: first-round PCR. The PCR products were then extracted from a 0.8% agarose gel via a QIAquick Gel Extraction Kit (Qiagen Inc.) and used for scFv library construction.

## Construction of phage-displayed scFv libraries

The phagemid vector pComb3XSS (kindly provided by Dr. Carlos Barbas, Scripps Research Institute, La Jolla, CA) and constructed scFvs were digested by the restriction endonuclease S*fi*I (New England Biolabs, Inc.) at 50°C for 16 hours to generate complementary cohesive ends. The 5' end of the digested pComb3XSS was dephosphorylated with Quick CIP (New England Biolabs, Inc.) at 37 °C for 30 min. The products were purified via a QIAquick Gel Extraction Kit (QIAgen Inc., Hilden, Germany). A total of 1.4 µg of purified-S*fi*I-digested-CIP pComb3XSS vector and 700 ng of purified-SfiI-digested scFv insert were ligated with T4 ligase (New England Biolabs, Inc.) at 16 °C for 16 h. The quantity and efficiency of each library were determined via colony counting and colony PCR techniques. Electrocompetent TG1 *E. coli* cells were transformed with individual scFv libraries. Phagemids were rescued by the addition of $1 \times 10^{11}$ pfu of VCSM13 helper phage (Stratagene, La Jolla, CA, USA). Phage libraries were precipitated via PEG/NaCl and stored in PBS containing 1% (w/v) BSA. TG1 (OD600 = 0.5–0.6) was used for determining phage library size by counting colony-forming units on ampicillin-impregnated LB plates.

## Biopanning (Affinity selection)

The pooled scFv-phage clones with high binding affinity from the libraries were selected by a biopanning assay for 4 rounds. For each round, 500 ng of antigen was immobilized in each duplicate well of a microtiter plate (Thermo Fisher Scientific, Rochester, NY, USA) with 100 µl of coating buffer and incubated at 4 °C for 16 h.

We used 2 kinds of target antigens: purified recombinant rabies virus glycoprotein (RABV-G) and purified inactivated rabies virus (RABV). The recombinant glycoprotein of the rabies virus was expressed via a Bac-to-Bac baculovirus expression system in High Five insect cells. It was purified via immobilized metal affinity chromatography. The inactivated rabies virus was prepared as described previously[87]. The rabies virus RABV/TH/SQ382/2010 (GenBank accession number ON808418) was originally isolated from the brain of a rabid dog by Dr. Boonlert Lumlertdacha (Queen Saovabha Memorial Institute, Bangkok, Thailand). It was propagated in mouse brains for seven passages and adapted to BHK21. C13 cells for five passages. The virus working stock was inactivated at 56 °C for 30 min. The virus originated from a Thai rabies strain provided by Dr. Boonlert Lumlertdacha (Queen Saovabha Memorial Institute, Bangkok, Thailand). The virus was isolated from the brain of a rabid dog, propagated in mouse brains for seven passages, and increased virus titers were detected in BHK21. C13 cells for five passages.

Next, the coated wells were blocked with 5% (w/v) skim milk (SM) in TBS/T blocking buffer for 2 h at 37 °C. During this step, the subtraction method was performed by separately adding each scFv-phage library to 5% SM (without antigen) coated well and incubated at 37 °C for 1 h. The SM-unbound phages were subsequently harvested via gentle pipetting. After that, the blocking buffer was shaken from the antigen-coated wells, and 100 µl/well of BSA-unbound phage libraries from the subtraction step were then incubated with individual antigens at 37 °C for 2 h. Unbound phages were then removed by immediate washing with 0.05% (v/v) Tween 20 in TBS (0.05% TBS-T). Bound phages were eluted with 10 mg/ml trypsin in TBS elution buffer for 30 min at 37 °C. Eluates (select-pooled phage clones) were then used to infect TG1 *E. coli* cells. The enriched phagemids were rescued via VCSM13 helper phage (Stratagene, La Jolla, CA, USA), and Ag-specific enriched phages were amplified overnight. Amplified phages were titered and used as the input phage for the next consecutive round of panning. The input and output (eluate) phage titers were calculated via colony counting. After the 4th round of panning, the input and output phage clones were analyzed individually for rabies virus glycoprotein protein-specific scFv by ELISA. The biopanning assay strategy is shown in Table 5.

*Specific binding ELISA of individual clones*

To prepare the samples for ELISA, overnight cultures of individual selected clones were grown in 3 ml of 2XYT media, and protein expression was induced with 0.5 mM IPTG when the $OD_{600}$ reached 0.5–0.6. The cultures were then incubated at 37 °C for 16 h and lysed via sonication. The cell lysates were subsequently centrifuged at 22,000 ×g for 15 min. The supernatants were harvested and stored at -20 °C until ELISA was performed.

| Round | Antigen | Input phage | Washing step |
|---|---|---|---|
| 1 | 500 ng/well | 100 µl/well x2 wells, 2 h | 10 rounds, 5 min/round |
| 2 | 500 ng/well | 100 µl/well x2 wells, 2 h | 10 rounds, 5 min/round |
| 3 | 500 ng/well | 100 µl/well, 2 h | 5 rounds, 5 min/round |
| 4 | 500 ng/well | 100 µl/well, 2 h | 5 rounds, 5 min/round |

**Table 5**. Biopanning selection strategy.

To prepare the ELISA for each sample, 500 ng/well RABV-G and RABV were incubated on microtiter plates at 4 °C overnight. The next day, the wells were blocked with 5% skim milk in PBS-T for 2 h at 37 °C. SM was used as a negative control. The expression control was defined as the scFv expression of each selected sample determined by scFv binding to the bottom of the empty wells. Next, 100 µl of undiluted supernatant was added to each well and incubated for 1 h at 37 °C. The wells were washed with 0.05% PBS-T 5 times. Anti-6X HIS and HRP (clone HIS-1, #A7058, UK) in washing buffer at a dilution of 1:2000 was used for detection of the antigen-bound antibody in the sample, which was subsequently incubated for 1 h at 37 °C. Then, the wells were repeatedly washed, and the bound antibody was detected with 100 µl/well TMB peroxidase substrate (Thermo Fisher Scientific, Rochester, NY, USA). The absorbance at 450 nm was measured via a spectrophotometer.

## DNA sequencing, amino acid translation and CDR annotations

Individual ELISA-positive phage clones were subjected to plasmid isolation via the FavorPrep Plasmid DNA Extraction Mini Kit (Favorgen Biotech, Pingtung, Taiwan). Purified plasmids containing 800–850 bp inserts were used to determine the DNA sequences via Sanger sequencing via the pComb3XSS sequencing primers OmpA and DpSeq, as shown in Table 4. The sequences were analyzed to identify open reading frames (ORFs) and translated into amino acid sequences via the web-based program ExPASy translate tool (https://web.ExPASy.org/translate/). The DNA sequences of the scFvs were analyzed on the basis of canine immunoglobulin databases via the IMGT/V-QUEST online tool (https://www.imgt.org/IMGT_vquest/input). The complementary determining regions (CDRs), framework regions (FRs), germline allele use, mutations, and other regions of each sequenced VH and VL chain (both λ and κ) were subsequently annotated.

*Soluble protein expression of pComb3XSS harboring a canine scFv antibody*

Individual pComb3XSS phagemid vectors harboring canine scFv genes were transformed into *E. coli* BL21 Gold (DE3) cells (Agilent Technology, USA) via the heat-shock method according to the manufacturer's protocol. A 10-mL overnight culture of the transformants was conducted at 37 °C. The next day, the overnight cultures were used as the starter for 1 L of culture and incubated at 37 °C for 2–3 h. When the $OD_{600}$ reached 0.5–0.6, IPTG was added to the culture at a final concentration of 0.5 mM, and the mixture was incubated at 30 °C for 16 h. The 1 L-induced culture mixture was transferred to a 250-ml centrifuge bottle and centrifuged at 5000×*g* for 30 min each. The media supernatant was discarded, and the cell pellet was washed once with 100 ml of sterilized 1X PBS after the last round of culture centrifugation. Finally, the PBS was rinsed out, and the pellet was completely dried by inverting the bottle on paper. The completely dried pellet was subsequently stored at − 80 °C until use.

*Purification of soluble scFv antibodies*

The pellets were dissolved and chemically lysed with 50 ml of native lysis buffer with 1 mg/ml lysozyme, 1% NP-40, and protease inhibitors. Then, the dissolved pellets were further lysed by sonication on ice. The supernatants were harvested into 50-ml tubes. The HIS-trap FF column (Cytiva) was applied to BioRad NGC Medium-Pressure Liquid Chromatography System according to the manufacturer's recommended protocol to purify the protein from the supernatant. The flow-through and washing fractions were collected. After, the binding buffer was adjusted by gradually increasing the imidazole concentration. To determine the purity and existence of scFv protein in the elution fractions, SDS-PAGE analysis and Western blotting were performed with the elution fractions, showing a high peak absorbance at 280 nm in the NGC graph. Then, the scFv concentration from each elution was measured using Amicon ultrafiltration methods. The antibody concentrations were measured using a Pierce BCA Protein Assay Kit (Thermo Scientific), and the absorbance at 560 nm was interpreted.

*Measurement of viral neutralization activity (VNA) via the modified rapid fluorescent foci inhibition test (RFFIT)*

RFFIT was performed for the detection of anti-RABV neutralizing antibodies, either in serum or soluble scFvs expressed by *E. coli*. In brief, 50 µl of tenfold serial dilutions of heat-inactivated immunized serum or twofold serial dilutions of purified scFv were incubated with 50 µl of the CVS-11 rabies virus strain in 96-well tissue culture plates for 90 min at 37 °C with 5% $CO_2$. Fifty microliters of twofold dilutions of 1 IU/ml WHO standard anti-RABV immunoglobulin (RAI), positive control (1 IU/ml and 10 IU/ml ERIG) and negative control (heat-inactivated normal serum) were also performed via the same methods as those used in the sample wells. All the samples, standards, controls, and viruses (titers ranged from 30 to 100 $TCID_{50}$/well), and the cells were diluted in 2% DMEM. Fifty microliters of $10^5$ BHK-21(C13) cells/ml were added to the sample-virus and control-virus mixtures and incubated for an additional 21 h at 37 °C with 5% $CO_2$. After that, all media were rinsed out from the examined wells, fixed in 90% acetone for 5 minutes, and air dried. The viruses inside the cell were stained with a commercial antirabies (polyclonal) virus N-FITC-labeled conjugate at 37 °C with 5% $CO_2$ for 1 h. Eight distinct microscopic fields per well were examined via a fluorescence microscope to count the rabies virus-infected foci (green foci). The number of virus-negative fields per well was recorded, and the RFFIT titers were calculated via probit analysis. The endpoint VNA titer of the test serum was transformed into international units per mL (IU/mL) by calibrating the results against the neutralization endpoint titer ($TCID_{50}$) of the standard RAI.

## Bioinformatics

The protein sequences of the neutralizing scFv clones and rabies virus glycoprotein (RABV-G, SQ382, which was retrieved from Dr. Porntippa Lekchareonsuk) were uploaded to the SWISS-MODEL server (https://swissmodel.ExPASy.org/interactive) to find the best templates and create three-dimensional (3D) structure homology models determined by various parameters. The HADDOCK 2.4 web server (https://wenmr.science.uu.nl/haddock2.4/submit/1) was used for in silico docking simulations between the best homology models of scFv and RABV-G (SQ382). The PDB-simulated structures of K9RABVscFv and RABV-G (SQ382) were submitted to the server as input data for molecules no. 1 and 2, respectively. The amino acids on CDR1-3 of both the VH and VL of the

scFv were implemented as the active residues of molecule no. 1. The active residues of molecule no. 2 were the amino acids on the antigenic sites of RABV-G that were previously reported in databases and publications (see the literature review) 62,71. Parameter values of the default setting were used. Once the docking processes were completely interpreted, the best prediction models of the complexes were selected on the basis of the smallest HADDOCK scores. The binding affinity (ΔG) and dissociation constant (Kd) were predicted via the PRODIGY web server (https://bianca.science.uu.nl/prodigy/). The best docking PDB models of these 2 complexes were then visualized via BIOVIA Discovery Studio 2021 software. Moreover, the interactions between residues of the scFv/RABV-G complexes were also observed via this software.

## Data availability

Primer sequences in "Table 4. The set of primers based on the pComb3XSS phagemid for canine VH and VL chains and scFv amplification, including sequencing primers, were retrieved from Braganza et al. (2011).2) The RABV-G (SQ382) protein sequence and bioinformatics data are provided in the supplementary information file.The RABV-G (SQ382) nucleotide sequence data are available from the GenBank accession number ON808418.3) All protein structure data used as 3D templates for homology model prediction in this study have been deposited in the Worldwide Protein Data Bank (wwPDB):3.1 PDBID no. 8DY2.1. A (human GLK1 spFv) was used as a template for K9RABVscFv1. DOI: https://doi.org/10.2210/pdb8DY2/pdb3.2 PDBID no. 1×9Q (human anti-fluorescein scFv) was used as a template for K9RABVscFv16.DOI: https://doi.org/10.2210/pdb1×9Q/pdb3.3 PDBID no. 7U9G (monomer form of RABV-G) was used as a template for RABV-G (SQ382). DOI: https://doi.org/10.2210/pdb7U9G/pdb4) The amino acid sequences of K9RABVscFv1, 2, 12, 15, and 16 are currently under the process of patent registration (patent filing number 2401005189) assigned by the Thailand Department of Intellectual Property (DIP).

Received: 23 May 2024; Accepted: 16 September 2024
Published online: 03 October 2024

## References

1. Thanapongtharm, W., Suwanpakdee, S., Chumkaeo, A., Gilbert, M. & Wiratsudakul, A. Current characteristics of animal rabies cases in Thailand and relevant risk factors identified by a spatial modeling approach. *PLoS Negl. Trop. Dis.* **15**, e0009980. https://doi.org/10.1371/journal.pntd.0009980 (2021).
2. Niezgoda, M., Hanlon, C. A. & Rupprecht, C. E. Animal rabies. *Rabies* 163–218 (2003).
3. Dietzschold, B., Tollis, M., Lafon, M., Wunner, W. H. & Koprowski, H. Mechanisms of Rabies virus neutralization by glycoprotein-specific monoclonal antibodies. *Virology* **161**, 29–36 (1987).
4. Callaway, H. M. et al. Structure of the Rabies virus glycoprotein trimer bound to a prefusion-specific neutralizing antibody. *Sci. Adv.* **8**, eabp9151. https://doi.org/10.1126/sciadv.abp9151 (2022).
5. Flamand, V. et al. Vaccination with tumor-antigen-pulsed dendritic cells induces in vivo resistance to a B cell lymphoma. *Adv. Exp. Med. Biol.* **329**, 611–616. https://doi.org/10.1007/978-1-4615-2930-9_102 (1993).
6. Prehaud, C., Coulon, P., LaFay, F., Thiers, C. & Flamand, A. Antigenic site II of the Rabies virus glycoprotein: structure and role in viral virulence. *J. Virol.* **62**, 1–7. https://doi.org/10.1128/JVI.62.1.1-7.1988 (1988).
7. Seif, I., Coulon, P., Rollin, P. E. & Flamand, A. Rabies virulence: effect on pathogenicity and sequence characterization of Rabies virus mutations affecting antigenic site III of the glycoprotein. *J. Virol.* **53**, 926–934. https://doi.org/10.1128/JVI.53.3.926-934.1985 (1985).
8. Yang, F. et al. Structural analysis of rabies virus glycoprotein reveals pH-dependent conformational changes and interactions with a neutralizing antibody. *Cell Host Microbe* **27**, 441–453. https://doi.org/10.1016/j.chom.2019.12.012 (2020).
9. Tenzin & Ward, M. Review of rabies epidemiology and control in South, South East and East Asia: past, present and prospects for elimination. *Zoonoses Public. Health* **59**, 451–467 (2012).
10. World Health Organization (WHO) (2020).
11. Hampson, K. et al. Estimating the global burden of endemic canine rabies. *PLoS Negl. Trop. Dis.* **9**, e0003709 (2015).
12. Townsend, S. E. et al. Surveillance guidelines for disease elimination: a case study of canine rabies. *Comp. Immunol. Microbiol. Infect. Dis.* **36**, 249–261 (2013).
13. Leung, T. & Davis, S. A. Rabies vaccination targets for stray dog populations. *Front. Veterinary Sci.* **4**, 52 (2017).
14. Kasempimolporn, S. et al. Prevalence of Rabies virus infection and rabies antibody in stray dogs: A survey in Bangkok, Thailand. *Prev. Vet. Med.* **78**, 325–332 (2007).
15. Rupprecht, C. E., Fooks, A. R. & Abela-Ridder, B. *Laboratory Techniques in Rabies* Vol. 1 (WHO, 2018).
16. Premashthira, S. et al. The impact of socioeconomic factors on knowledge, attitudes, and practices of dog owners on dog rabies control in Thailand. *Front. Veterinary Sci.* **8**, 699352 (2021).
17. Zhao, X. L., Yin, J., Wang, H., Jiang, M. & Hou, X. J. Construction of human phage-displayed scFv library and selection of the ScFv against Rabies virus. *Xi Bao Yu Fen Zi Mian Yi Xue Za Zhi* **20**, 243–247 (2004).
18. Sun, L. et al. Generation and characterization of neutralizing human recombinant antibodies against antigenic site II of Rabies virus glycoprotein. *Appl. Microbiol. Biotechnol.* **96**, 357–366. https://doi.org/10.1007/s00253-012-4171-4 (2012).
19. Sparrow, E. et al. Recent advances in the development of monoclonal antibodies for rabies post exposure prophylaxis: a review of the current status of the clinical development pipeline. *Vaccine* **37**(Suppl 1), A132–A139. https://doi.org/10.1016/j.vaccine.2018.11.004 (2019).
20. Serum Institute of India PVT. LTD (2018).
21. Yumoto, K. et al. Characterization of single-chain fv fragments of neutralizing antibodies to rabies virus glycoprotein. *Viruses* **13**https://doi.org/10.3390/v13112311 (2021).
22. Terryn, S., Francart, A., Rommelaere, H., Stortelers, C. & Van Gucht, S. Post-exposure treatment with anti-rabies VHH and vaccine significantly improves Protection of mice from Lethal rabies infection. *PLoS Negl. Trop. Dis.* **10**, e0004902. https://doi.org/10.1371/journal.pntd.0004902 (2016).
23. Sun, L., Liu, Y., Li, C., Li, D. & Liang, M. Generation of human ScFv antibodies for antigenic site III of rabies virus glycoprotein from antibody-phage libraries by Chain Shuffling. *Bing Du Xue Bao* **32**, 393–398 (2016).
24. Boucher, L. E. et al. Stapling scFv for multispecific biotherapeutics of superior properties. *MAbs* **15**, 2195517. https://doi.org/10.1080/19420862.2023.2195517 (2023).
25. Midelfort, K. S. et al. Substantial energetic improvement with minimal structural perturbation in a high affinity mutant antibody. *J. Mol. Biol.* **343**, 685–701. https://doi.org/10.1016/j.jmb.2004.08.019 (2004).

26. Miandehi, N., Bidoki, S., Ajorloo, M. & Gholami, A. Change in the Basic structure of the rabies Virus Glycoprotein by Reverse Genetics. *Iran. J. Med. Microbiol.* **14**, 348–360. https://doi.org/10.30699/ijmm.14.4.348 (2020).
27. Shi, C. et al. Research progress on neutralizing epitopes and antibodies for the rabies virus. *Infect. Med.* (2022).
28. Zhao, X. L. et al. Generation and characterization of human monoclonal antibodies to G5, a linear neutralization epitope on glycoprotein of Rabies virus, by phage display technology. *Microbiol. Immunol.* **52**, 89–93. https://doi.org/10.1111/j.1348-0421.2008.00016.x (2008).
29. World Health Organization (WHO) (2018).
30. World Health Organization (WHO) (2014).
31. McClain, J. B., Chuang, A., Reid, C., Moore, S. M. & Tsao, E. Rabies virus neutralizing activity, pharmacokinetics, and safety of the monoclonal antibody mixture SYN023 in combination with rabies vaccination: results of a phase 2, randomized, blinded, controlled trial. *Vaccine* **39**, 5822–5830. https://doi.org/10.1016/j.vaccine.2021.08.066 (2021).
32. Bunn, T., Ridpath, H. & Beard, P. *The Relationship Between Rabies Antibody Titers in Dogs and Cats and Protection from Challenge* (Centers Disease Control, 1984).
33. Rabies, F. Developing monoclonal antibody cocktails for the passive immunization component of post-exposure prophylaxis. *Guidance for Industry* (2021).
34. Fan, L., Zhang, L., Li, J. & Zhu, F. Advances in the progress of monoclonal antibodies for rabies. *Hum. Vaccines Immunother.* **18**, 2026713 (2022).
35. World Health Organization (WHO). *Rabies Vaccines and Immunoglobulins: WHO Position: Summary of 2017 Updates* (WHO, 2018).
36. Andris-Widhopf, J., Steinberger, P., Fuller, R., Rader, C. & Barbas, C. F. Generation of human Fab antibody libraries: PCR amplification and assembly of light- and heavy-chain coding sequences. *Cold Spring Harb Protoc*. https://doi.org/10.1101/pdb.prot065565 (2011).
37. Pruksametanan, N. *Production of human monoclonal antibodies against rabies virus using phage display technology (Doctoral dissertation)* (School of Biotechnology Institute of Agricultural Technology, Suranaree University of Technology, 2013).
38. Pansri, P., Jaruseranee, N., Rangnoi, K., Kristensen, P. & Yamabhai, M. A compact phage display human scFv library for selection of antibodies to a wide variety of antigens. *BMC Biotechnol.* **9**, 6. https://doi.org/10.1186/1472-6750-9-6 (2009).
39. Aavula, S. M. et al. Generation and characterization of an scFv Directed against Site II of rabies glycoprotein. *Biotechnol Res Int* 652147. https://doi.org/10.4061/2011/652147 (2011).
40. Kumar, R. et al. A novel strategy for efficient production of anti-V3 human scFvs against HIV-1 clade C. *BMC Biotechnol.* **12**, 87. https://doi.org/10.1186/1472-6750-12-87 (2012).
41. Braganza, A. et al. Generation and validation of canine single chain variable fragment phage display libraries. *Vet. Immunol. Immunopathol.* **139**, 27–40. https://doi.org/10.1016/j.vetimm.2010.07.026 (2011).
42. Chiang, Y. L., Sheng-Dong, R., Brow, M. A. & Larrick, J. W. Direct cDNA cloning of the rearranged immunoglobulin variable region. *Biotechniques* **7**, 360–366 (1989).
43. Yamanaka, H. I. & Inoue, T. Ikeda-Tanaka, O. Chicken monoclonal antibody isolated by a phage display system. *J. Immunol.* **157**, 1156–1162 (1996).
44. Davies, E. L. et al. Selection of specific phage-display antibodies using libraries derived from chicken immunoglobulin genes. *J. Immunol. Methods* **186**, 125–135. https://doi.org/10.1016/0022-1759(95)00143-x (1995).
45. Andris-Widhopf, J., Rader, C., Steinberger, P., Fuller, R. & Barbas, C. F. Methods for the generation of chicken monoclonal antibody fragments by phage display. *J. Immunol. Methods* **242**, 159–181. https://doi.org/10.1016/s0022-1759(00)00221-0 (2000).
46. Sepulveda, J. & Shoemaker, C. B. Design and testing of PCR primers for the construction of scFv libraries representing the immunoglobulin repertoire of rats. *J. Immunol. Methods* **332**, 92–102. https://doi.org/10.1016/j.jim.2007.12.014 (2008).
47. Ridder, R., Schmitz, R., Legay, F. & Gram, H. Generation of rabbit monoclonal antibody fragments from a combinatorial phage display library and their production in the yeast *Pichia pastoris*. *Biotechnol. (N Y)* **13**, 255–260. https://doi.org/10.1038/nbt0395-255 (1995).
48. Steinberger, P., Sutton, J. K., Rader, C., Elia, M. & Barbas, C. F. Generation and characterization of a recombinant human CCR5-specific antibody. A phage display approach for rabbit antibody humanization. *J. Biol. Chem.* **275**, 36073–36078. https://doi.org/10.1074/jbc.M002765200 (2000).
49. Scripps Research (2020).
50. Rader, C., Cheresh, D. A. & Barbas, C. F. 3rd. A phage display approach for rapid antibody humanization: designed combinatorial V gene libraries. *Proc. Natl. Acad. Sci. USA* **95**, 8910–8915. https://doi.org/10.1073/pnas.95.15.8910 (1998)
51. Popkov, M. et al. Rabbit immune repertoires as sources for therapeutic monoclonal antibodies: the impact of kappa allotype-correlated variation in cysteine content on antibody libraries selected by phage display. *J. Mol. Biol.* **325**, 325–335. https://doi.org/10.1016/s0022-2836(02)01232-9 (2003).
52. Pan, Y. et al. Screening of potent neutralizing antibodies against SARS-CoV-2 using convalescent patients-derived phage-display libraries. *Cell Discov.* **7**, 57. https://doi.org/10.1038/s41421-021-00295-w (2021).
53. Ray, K., Embleton, M. J., Jailkhani, B. L., Bhan, M. K. & Kumar, R. Selection of single chain variable fragments (scFv) against the glycoprotein antigen of the Rabies virus from a human synthetic scFv phage display library and their fusion with the fc region of human IgG1. *Clin. Exp. Immunol.* **125**, 94–101. https://doi.org/10.1046/j.1365-2249.2001.01515.x (2001).
54. Ando, T., Yamashiro, T., Takita-Sonoda, Y., Mannen, K. & Nishizono, A. Construction of human Fab library and isolation of monoclonal fabs with rabies virus-neutralizing ability. *Microbiol. Immunol.* **49**, 311–322. https://doi.org/10.1111/j.1348-0421.2005.tb03735.x (2005).
55. Kramer, R. A. et al. The human antibody repertoire specific for Rabies virus glycoprotein as selected from immune libraries. *Eur. J. Immunol.* **35**, 2131–2145. https://doi.org/10.1002/eji.200526134 (2005).
56. Liu, X. et al. Characterization of a human antibody fragment Fab and its calcium phosphate nanoparticles that inhibit rabies virus infection with vaccine. *PLoS ONE* **6**, e19848. https://doi.org/10.1371/journal.pone.0019848 (2011).
57. Pitaksajjakul, P. et al. Fab MAbs specific to HA of influenza virus with H5N1 neutralizing activity selected from immunized chicken phage library. *Biochem. Biophys. Res. Commun.* **395**, 496–501. https://doi.org/10.1016/j.bbrc.2010.04.040 (2010).
58. Lee, C. H. et al. The bottlenecks of preparing Virus particles by size exclusion for antibody generation. *Int. J. Mol. Sci.*. https://doi.org/10.3390/ijms232112967 (2022).
59. Reiche, N. et al. Generation and characterization of human monoclonal scFv antibodies against *Helicobacter pylori* antigens. *Infect. Immun.* **70**, 4158–4164. https://doi.org/10.1128/IAI.70.8.4158-4164.2002 (2002).
60. Lee, W., Syed, A. A., Leow, C. Y., Tan, S. C. & Leow, C. H. Isolation and characterization of a novel anti-salbutamol chicken scFv for human doping urinalysis. *Anal. Biochem.* **555**, 81–93. https://doi.org/10.1016/j.ab.2018.05.009 (2018).
61. Wang, F. et al. Generation and functional analysis of single chain variable fragments (scFvs) targeting the nucleocapsid protein of porcine epidemic diarrhea virus. *Appl. Microbiol. Biotechnol.* **106**, 995–1009. https://doi.org/10.1007/s00253-021-11722-z (2022).
62. Li, C. et al. Construction and screening of human immunized phage-display antibody libraries against Rabies virus. *Acta Univ. Med. Nanjing (Natural Sci)* **30**, 575–578 (2010).
63. Hultberg, A. et al. Llama-derived single domain antibodies to build multivalent, superpotent and broadened neutralizing anti-viral molecules. *PLoS One.* **6**, e17665. https://doi.org/10.1371/journal.pone.0017665 (2011).
64. Zhang, Y. In *MAbs.* 2213793 (Taylor & Francis).

65. Bao, Y., Guo, Y., Xiao, S. & Zhao, Z. Molecular characterization of the VH repertoire in Canis familiaris. *Vet. Immunol. Immunopathol.* **137**, 64–75. https://doi.org/10.1016/j.vetimm.2010.04.011 (2010).
66. Bernat, N. V. *Definition of Immunoglobulin Germline Genes by Next Generation Sequencing for Studies of Antigen-Specific B Cell Responses* (Karolinska Institutet (Sweden), 2019).
67. Cullen, J. N. et al. Development and application of a next-generation sequencing protocol and bioinformatics pipeline for the comprehensive analysis of the canine immunoglobulin repertoire. *PLoS ONE* **17**, e0270710. https://doi.org/10.1371/journal.pone.0270710 (2022).
68. Steiniger, S. C. et al. Fundamental characteristics of the expressed immunoglobulin VH and VL repertoire in different canine breeds in comparison with those of humans and mice. *Mol. Immunol.* **59**, 71–78. https://doi.org/10.1016/j.molimm.2014.01.010 (2014).
69. Arndt, K. M., Müller, K. M. & Plückthun, A. Factors influencing the dimer to monomer transition of an antibody single-chain fv fragment. *Biochemistry* **37**, 12918–12926. https://doi.org/10.1021/bi9810407 (1998).
70. Hudson, P. J. & Kortt, A. A. High avidity scFv multimers; diabodies and triabodies. *J. Immunol. Methods* **231**, 177–189 (1999).
71. Le Gall, F., Kipriyanov, S. M., Moldenhauer, G. & Little, M. Di-, tri-and tetrameric single chain fv antibody fragments against human CD19: effect of valency on cell binding. *FEBS Lett.* **453**, 164–168 (1999).
72. Arslan, M. et al. Effect of non-repetitive linker on in vitro and in vivo properties of an anti-VEGF scFv. *Sci. Rep.* **12**, 5449 (2022).
73. Quintero-Hernández, V. et al. The change of the scFv into the Fab format improves the stability and in vivo toxin neutralization capacity of recombinant antibodies. *Mol. Immunol.* **44**, 1307–1315. https://doi.org/10.1016/j.molimm.2006.05.009 (2007).
74. Röthlisberger, D., Honegger, A. & Plückthun, A. Domain interactions in the Fab Fragment: A comparative evaluation of the single-chain fv and Fab Format Engineered with Variable domains of different Stability. *J. Mol. Biol.* **347**, 773–789. https://doi.org/10.1016/j.jmb.2005.01.053 (2005).
75. Zhao, X. L. et al. Selection and affinity maturation of human antibodies against Rabies virus from a scFv gene library using ribosome display. *J. Biotechnol.* **144**, 253–258. https://doi.org/10.1016/j.jbiotec.2009.09.022 (2009).
76. Muller, T. et al. Development of a mouse monoclonal antibody cocktail for post-exposure rabies prophylaxis in humans. *PLoS Negl. Trop. Dis.* **3**, e542. https://doi.org/10.1371/journal.pntd.0000542 (2009).
77. Kim, P. K. et al. A broad-spectrum and highly potent human monoclonal antibody cocktail for rabies prophylaxis. *PLoS ONE* **16**, e0256779. https://doi.org/10.1371/journal.pone.0256779 (2021).
78. Hellert, J. et al. Structure of the prefusion-locking broadly neutralizing antibody RVC20 bound to the Rabies virus glycoprotein. *Nat. Commun.* **11**, 596. https://doi.org/10.1038/s41467-020-14398-7 (2020).
79. Gogtay, N. J. et al. Comparison of a Novel human rabies monoclonal antibody to human rabies immunoglobulin for Postexposure Prophylaxis: a phase 2/3, Randomized, Single-Blind, Noninferiority, controlled study. *Clin. Infect. Dis.* **66**, 387–395. https://doi.org/10.1093/cid/cix791 (2018).
80. Bakker, A. B. et al. First administration to humans of a monoclonal antibody cocktail against Rabies virus: safety, tolerability, and neutralizing activity. *Vaccine* **26**, 5922–5927. https://doi.org/10.1016/j.vaccine.2008.08.050 (2008).
81. Sun, L., Liu, Y., Li, C., Li, D. & Liang, M. [Development of recombinant human monoclonal antibody cocktail for post-exposure rabies Prophylaxis]. *Bing Du Xue Bao* **32**, 399–403 (2016).
82. Chao, T. Y. et al. SYN023, a novel humanized monoclonal antibody cocktail, for post-exposure prophylaxis of rabies. *PLoS Negl. Trop. Dis.* **11**, e0006133. https://doi.org/10.1371/journal.pntd.0006133 (2017).
83. De Benedictis, P. et al. Development of broad-spectrum human monoclonal antibodies for rabies post-exposure prophylaxis. *EMBO Mol. Med.* **8**, 407–421. https://doi.org/10.15252/emmm.201505986 (2016).
84. Papaneri, A. B., Wirblich, C., Marissen, W. E. & Schnell, M. J. Alanine scanning of the Rabies virus glycoprotein antigenic site III using recombinant rabies virus: implication for post-exposure treatment. *Vaccine* **31**, 5897–5902. https://doi.org/10.1016/j.vaccine.2013.09.038 (2013).
85. Chao, T. Y., Zhang, S. F., Chen, L., Tsao, E. & Rupprecht, C. E. In vivo efficacy of SYN023, an anti-rabies monoclonal antibody cocktail, in Post-exposure Prophylaxis Animal models. *Trop. Med. Infect. Dis.***5**https://doi.org/10.3390/tropicalmed5010031 (2020).
86. Tuffereau, C. et al. Arginine or lysine in position 333 of ERA and CVS glycoprotein is necessary for rabies virulence in adult mice. *Virology* **172**, 206–212. https://doi.org/10.1016/0042-6822(89)90122-0 (1989).
87. Tanwattana, N. et al. Human BST2 inhibits Rabies virus release independently of cysteine-linked dimerization and asparagine-linked glycosylation. *Plos ONE* **18**, e0292833 (2023).


## Acknowledgements

This research was funded by (1) National Research Council of Thailand (NRCT) and Kasetsart University (KU), grant number N42A670624. (2) Research and Researchers for Industries (RRi) Ph.D. scholarships, grant number PHD60I0075 awarded by the National Research Council of Thailand (NRCT); (3) Research Scholarships for Graduate Students of Universities in Thailand, awarded by The KING PRAJADHIPOK and QUEEN RAMBHAIBARNI MEMORIAL FOUNDATION. We would like to sincerely thank the dogs' owners and all the dogs used for the sample collection. Special thanks to JICA, who kindly provided the budget for laboratory equipment that was used in this study.

## Author contributions

Conceptualization, P.R., P.P., P.L., A.C., S.B., U.B., K.L. ; methodology, A.C., P.C., W.S., W.P., and I.P.; Software, A.C., U.B., and S.T.; validation, A.C., P.P. and P.L. ; formal analysis, P.R.; investigation, A.C. ; resources, P.R., P.P., P.L., W.P., A.H. ; data curation, P.R., P.P., P.L.; writing—original draft preparation, A.C. ; writing-review and editing, P.R., S.B., and P.P.; visualization, A.C., S.T., P.L., P.P. and P.R.; supervision, P.R., P.L., P.P., and A.H.; project administration, P.L., and P.R. ; funding acquisition, P.L. All authors have read and agreed to the published version of the manuscript.

## Declarations

## Competing interests

The authors declare no competing interests.

## Additional information

**Supplementary Information** The online version contains supplementary material available at https://doi.org/10.1038/s41598-024-73339-2.

**Correspondence** and requests for materials should be addressed to P.R.